
Cluster Frequency Conformal Prediction for Local Coverage

Tomer Lavi

Institute of Applied AI Research (AAIR)
Faculty of Computer and Information Science
Ben-Gurion University of the Negev, Beer-Sheva 84105, ISRAEL
tomerlav@post.bgu.ac.il

Bracha Shapira

Institute of Applied AI Research (AAIR)
Faculty of Computer and Information Science
Ben-Gurion University of the Negev, Beer-Sheva 84105, ISRAEL
bshapira@bgu.ac.il

Nadav Rappoport

Institute for Interdisciplinary Computational Science (ICS)
Faculty of Computer and Information Science
Ben-Gurion University of the Negev, Beer-Sheva 84105, ISRAEL
nadavrap@bgu.ac.il

Abstract

Conformal prediction provides distribution-free coverage guarantees, but in many-class classification it may still under-cover specific classes or subpopulations, preventing safe deployment in high-stakes applications. We propose Cluster Frequency Conformal Prediction (CFCP), a plug-in framework that adapts conformal prediction to local structure in a learned representation space. CFCP clusters learned embeddings, estimates cluster-level label-frequency distributions from calibration data, and for each test point constructs a sample-specific probability vector by softly mixing nearby cluster distributions regularized with global-prior and reliability-aware shrinkage. This vector is then conformalized using standard set constructors. In the disjoint-split regime, CFCP inherits standard finite-sample marginal validity. Under additional assumptions, CFCP further admits a local-validity interpretation. Since representation clusters aggregate locally similar samples, their empirical class frequencies provide a stable estimate of local label ambiguity. Across image and text benchmarks, CFCP achieves the best class coverage in 15/16 dataset/score-family comparisons and a competitive prediction set size efficiency, with several settings substantially more efficient. Overall, our results show that cluster-frequency information provides an effective localized signal for improving classwise reliability in many-class conformal prediction.

1 Introduction

Conformal prediction (CP) provides finite-sample marginal coverage guarantees for set-valued predictions under exchangeability, a principled and widely adopted tool for uncertainty quantification in machine learning [Vovk et al., 2005, Angelopoulos and Bates, 2021]. Marginal validity alone, however, can mask substantial disparities: a method may attain the target overall coverage while still

under-covering specific classes or subpopulations. This issue is especially pronounced in many-class settings, where calibration data are sparse per class and the conditional label distribution may vary substantially across regions of the representation space.

In these settings, a single global prediction rule may be too coarse. Classwise or Mondrian conformal methods calibrate separately per label, but in many-class problems they can become unstable or overly conservative because each class receives only a limited number of calibration examples [Vovk, 2012, Ding et al., 2023]. A complementary direction localizes conformal prediction in feature space: neighborhood-based methods [Ghosh et al., 2023], subgroup mixture models [Zhang and Candès, 2024], and covariate-aware reweighting schemes [Hore and Barber, 2023, Gil et al., 2024]. All show that representation-aware adaptation can improve uncertainty quantification beyond globally calibrated procedures. Yet, to the best of our knowledge, no existing method directly uses local cluster-level label frequency distributions as the primary probabilistic signal for conformal set construction - the precise gap that this work addresses.

We build on the observation that learned representations often organize data into subpopulations with different label compositions (see Figure 1). Learned embeddings preserve the covariate geometry induced by the trained network and can capture within-class and cross-class subpopulations with distinct empirical label frequencies. A test point may lie in a region whose local ambiguity differs markedly from the global average, even when its base-model confidence appears similar to that of other points. This suggests that conformal prediction should adapt not only to a model’s output scores, but also to the local label structure of the point’s neighborhood in representation space. Such structure may reflect not only class-level ambiguity, but also finer within-class variation. This suggests a concrete design principle: rather than relying on a single global probability vector, a conformal method should estimate the local label distribution of a test point’s neighborhood and use it directly as the input to set construction.



Figure 1: Visual intuition for our proposed Cluster Frequency Conformal Prediction (CFCP) framework. Example clusters induced by learned image representations. Left: eight samples from a highly homogeneous cluster whose sampled members are all labeled horse. Right: eight samples of a label-heterogeneous cluster. Such clusters illustrate the CFCP intuition that nearby samples in representation space may exhibit different local label distributions, which CFCP uses to form sample-specific probability vectors before standard conformal set construction.

We therefore propose Cluster Frequency Conformal Prediction (CFCP), a plug-in conformal framework for classification. CFCP first clusters learned embeddings, then estimates cluster-level label frequency distributions from calibration data. For a new point, it retrieves nearby clusters, forms a soft mixture of their label distributions and regularizes that mixture with global priors and reliability-aware shrinkage. The resulting sample-specific probability vector is then passed to a standard conformal set constructor. Thus, CFCP preserves the standard conformal thresholding machinery while replacing the global probability vector with one that is locally adapted to representation-space structure. Interpretability is a natural byproduct: each prediction set is grounded in the label distribution of structurally similar training examples, making the uncertainty transparent and auditable.

This design also yields a clean validity interpretation. In the disjoint-split regime, where the local cluster-frequency model is estimated on one subset and the conformal threshold is calibrated on another, CFCP inherits the usual finite-sample marginal validity guarantee of split conformal prediction. Under additional assumptions, randomized Adaptive Prediction Sets (APS) [Romano et al., 2020] further admits a sharper local-validity interpretation. Our primary goal is practical: to improve classwise reliability in the many-class settings where purely global methods systematically hide coverage disparities, a regime where exact conditional validity guarantees are generally unattainable.

Empirically, CFCP is designed for the regime where classwise reliability is hardest: many classes, heterogeneous representation geometry and limited calibration data per class. Across image and text benchmarks, CFCP improves the fraction of classes that satisfy the target coverage level in 15/16 within score-family comparisons against strong baselines, while maintaining competitive prediction-set sizes and, in several settings, substantially improving efficiency. This suggests that local cluster-frequency information can improve the tradeoff between classwise coverage and practical prediction-set size.

Our contributions are:

- We introduce CFCP, a plug-in conformal framework that constructs a sample-specific label distribution from cluster-level label frequencies in a learned representation space. CFCP provides both a computational and a statistical advantage over point-neighborhood methods in the many-class, high-dimensional regime.
- We show that CFCP inherits standard finite-sample marginal validity in the disjoint-split regime and we provide an oracle local-validity interpretation for randomized APS.
- We empirically show on challenging many-class image and text benchmarks that CFCP often improves classwise coverage while remaining competitive in set size.

1.1 Background and Related Work

Let $\{(X_i, Y_i)\}_{i=1}^m$ be exchangeable, let a base predictor be trained on a proper training split and let a nonconformity score $s : \mathcal{X} \times \mathcal{Y} \rightarrow \mathbb{R}$ quantify how atypical a candidate label is for a feature vector. In split conformal prediction (Split), calibration scores are computed on a held-out set $s_i = s(X_i, Y_i)$ for $i \in [m]$. Sort them as $s_{(1)} \leq \dots \leq s_{(m)}$ and set $\hat{q}_{1-\alpha} = s_{(k)}$, $k = \lceil (m+1)(1-\alpha) \rceil$. For a new x , the conformal prediction set is $\hat{c}(x) = \{y \in \mathcal{Y} : s(x, y) \leq \hat{q}_{1-\alpha}\}$. Then, the marginal coverage is $\mathbb{P}\{Y \in \hat{c}(X)\} \geq 1 - \alpha$.

Least Ambiguous Classifier (LAC) applies Split to the softmax score $1 - \hat{p}_x(y)$. It returns the set of labels whose predicted probability is at least the calibrated threshold $1 - \hat{q}_{1-\alpha}$. Adaptive set constructions such as APS, regularized APS (RAPS) and Sorted Adaptive Prediction Sets (SAPS) improve efficiency by using cumulative probability scores and rank-dependent regularization (Romano et al. [2020], Huang et al. [2023]). These methods are strong baselines, but they primarily target marginal validity and set size, not disparities in coverage across classes or subpopulations.

To address this, class-conditional and many-class conformal methods calibrate more finely across labels. Mondrian conformal prediction and Inductive Conformal Prediction (ICP) target label-conditional behavior [Vovk, 2012], while Ding et al. [2023] stabilize many-class classwise calibration by clustering labels with similar conformity-score distributions (CCP). Ding et al. [2025] further study classwise reliability in long-tailed classification by reweighting predicted probabilities of under-represented classes. Shi et al. [2024] follows CCP while improving efficiency by classwise label ranking (RC3P).

A complementary direction localizes conformal prediction in feature space. Neighborhood CP (NCP) uses nearby examples in a learned embedding space [Ghosh et al., 2023]. Posterior CP (PCP) models conformity scores through latent subgroup mixtures [Zhang and Candès, 2024], and recent work on local weighting and subgroup discovery further highlights the value of covariate-aware uncertainty quantification [Hore and Barber, 2023, Gil et al., 2024].

CFCP is most closely related to NCP and the local conformal literature, but differs fundamentally in both mechanism and robustness. NCP reweights the conformal quantile using per-point k-NN distances in the raw embedding space. This approach (i) scales as $O(n_{cal} \cdot d)$ per query, (ii) degrades in high dimensions as pairwise Euclidean distances concentrate and weights become nearly uniform, and (iii) provides no fallback when the neighborhood is uninformative. CFCP instead fits spherical k-means on ℓ_2 -normalized embeddings, compresses the calibration set into K centroids, and constructs a sample-specific label-frequency distribution, not a reweighted quantile, and reliability-aware shrinkage toward a global prior. This design reduces inference from $O(n_{cal} \cdot d)$ to $O(K \cdot d)$, exploits the angular geometry that supervised training imposes on the embedding space and gracefully degrades to standard conformal prediction when cluster assignments are diffuse.

2 Method

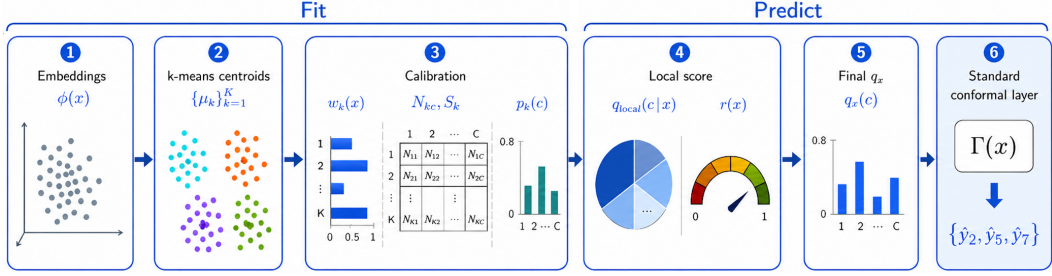


Figure 2: CFCP pipeline. Learned representations are clustered (1, 2) and calibration labels are accumulated as soft cluster counts (3). Smoothed cluster distributions are mixed according to the test point’s soft assignment weights and reliability-shrunk to form probabilities (4), which are passed to a standard conformal set constructor (5+6). See full notation list in Table 2 in the appendix.

CFCP has one core design choice: replace the global class-probability vector used by standard conformal set constructors with a locally adapted vector q_x , estimated from cluster-level label frequencies in representation space. This section formalizes that construction.

The method first clusters normalized learned representations and uses soft nearest-centroid assignments to estimate cluster-level label-frequency statistics from the calibration subset (Figure 2). These statistics are smoothed toward a global prior to obtain cluster distributions, which are then mixed according to the test point’s soft assignment weights. To avoid diffuse assignments or weakly supported clusters, CFCP applies reliability-aware shrinkage toward a fallback prior, producing the final sample-specific vector q_x . This vector is then passed to a standard conformal set constructor such as LAC, APS, RAPS, or SAPS.

2.1 Local cluster-frequency model

Let f be a pre-trained classifier over C classes, and let $\phi(x) \in \mathbb{R}^d$ be a fixed learned representation of input x . We ℓ_2 -normalize all embeddings and fit spherical k -means on the training representations, obtaining centroids $\mu_1, \dots, \mu_K \in \mathbb{R}^d$. For a point x with normalized embedding z , we identify its top- m nearest centroids by cosine similarity and convert their similarities $\delta_1(x), \dots, \delta_m(x)$ into soft assignment weights where $\tau > 0$ controls assignment sharpness. Lower values yield more local assignments.

$$w_j(x) = \frac{\exp(\delta_j(x)/\tau)}{\sum_{\ell=1}^m \exp(\delta_\ell(x)/\tau)}, \quad j = 1, \dots, m, \quad (1)$$

Let the calibration set be split into D_{stat} and D_q , where D_{stat} is used to estimate local label distributions and D_q is reserved for conformal quantile calibration. Rather than assigning each calibration point to a single cluster, CFCP distributes it fractionally across its m nearest centroids. Formally, the soft cluster-label counts are:

$$N_{kc} = \sum_{(x_i, y_i) \in D_{\text{stat}}} \sum_{j=1}^m w_{ij} \mathbf{1}\{k_j(x_i) = k, y_i = c\}, \quad (2)$$

together with effective cluster supports:

$$S_k = \sum_{(x_i, y_i) \in D_{\text{stat}}} \sum_{j=1}^m w_{ij} \mathbf{1}\{k_j(x_i) = k\}. \quad (3)$$

Thus, each calibration point contributes fractionally to several nearby clusters rather than to a single hard partition.

For each cluster k , we estimate a label distribution by shrinking the soft counts toward a global prior $\pi \in \Delta^{C-1}$:

$$\hat{p}_k(c) = \frac{N_{kc} + \beta \pi_c}{S_k + \beta}, \quad c = 1, \dots, C, \quad (4)$$

where $\beta > 0$ is a smoothing parameter. For a test point x , this yields the local cluster-frequency mixture

$$q_x^{\text{local}}(c) = \sum_{j=1}^m w_j(x) \hat{p}_{k_j(x)}(c), \quad c = 1, \dots, C. \quad (5)$$

Because this local mixture may be unreliable when assignments are diffuse or nearby clusters have low support, we further shrink it toward a fallback prior π_x , taken as the base model’s per-sample class-probability vector. We define a reliability weight: $\text{conf}(x) = \left(\max_{1 \leq j \leq m} w_j(x) \right)^\gamma$, $\text{sup}(x) = \sum_{j=1}^m w_j(x) S_{k_j(x)}$, $\text{supw}(x) = \frac{\text{sup}(x)}{\text{sup}(x) + \beta_{\text{sup}}}$, $r(x) = \text{conf}(x) \cdot \text{supw}(x) \in [0, 1]$, where $\gamma > 0$ controls the effect of assignment concentration and $\beta_{\text{sup}} > 0$ regularizes the neighborhood support term. $r(x)$ increases when the nearest centroid is dominant and those centroids are well-supported, otherwise we back off to the base model. The final CFCP probability vector is

$$q_x(c) = r(x) q_x^{\text{local}}(c) + (1 - r(x)) \pi_x(c), \quad c = 1, \dots, C. \quad (6)$$

2.2 Conformal prediction

CFCP separates local probability estimation from set construction. After computing q_x , we apply a standard split-conformal set constructor such as LAC, APS, RAPS or SAPS. Let $D_q = \{(x_i, y_i)\}_{i=1}^{n_q}$ denote the calibration subset reserved for quantile estimation, and let $s_i = s(x_i, y_i)$ be the induced nonconformity scores under the chosen constructor. The split-conformal threshold is $\hat{q}_{1-\alpha} = S_{(k)}$, $k = \lceil (n_q + 1)(1 - \alpha) \rceil$, where $S_{(k)}$ is the k -th order statistic.

For the Split score, the resulting prediction set is $\hat{\Gamma}(x) = \{c \in \{1, \dots, C\} : q_x(c) \geq 1 - \hat{q}_{1-\alpha}\}$. For APS, RAPS and SAPS, labels are sorted by $q_x(c)$ and included according to the corresponding cumulative or rank score rule. Hence, CFCP is a plug-in conformal framework: the only modification relative to standard conformal prediction is the construction of the probability vector q_x from local cluster-frequency information. Full score definitions for each constructor are given in Appendix A.

In the disjoint-split regime, where D_{stat} is used only to estimate the local model and D_q only for threshold calibration, CFCP inherits the standard finite-sample marginal validity guarantee. The formal theorem and proof are deferred to Appendix B.

3 Theoretical Analysis

CFCP is a plug-in conformal framework: it first estimates a local probability vector q_x from calibration-derived cluster statistics, and then applies a standard split-conformal threshold on a held-out calibration subset. We therefore distinguish between two levels of validity. First, in the disjoint-split regime $D_{\text{stat}} \cap D_q = \emptyset$, CFCP inherits the standard finite-sample marginal validity guarantee of split conformal prediction. Second, under additional assumptions, randomized APS admits an exact local validity statement. The oracle intuition follows the randomized oracle construction of Romano et al. [2020], while the set-valued oracle perspective is also consistent with Sadinle et al. [2019]. More broadly, this discussion fits the literature on conditional and local conformal validity, where exact local guarantees are known to require stronger structure or randomization [Vovk, 2012, Hore and Barber, 2023].

Appendix B provides the formal proofs for the following theorems and corollaries, the conditional-uniformity lemma underlying the oracle APS result and an approximate local-validity proposition for the general CFCP framework.

Theorem 1 (Finite-sample marginal validity of disjoint-split CFCP). *Assume the disjoint-split CFCP construction above: the local CFCP model is fitted without using labels from D_q , the calibration examples in D_q and the test point are exchangeable conditional on the fitted local model \widehat{M} , and any auxiliary randomization used by APS/RAPS/SAPS is independent. Let $\hat{\Gamma}$ be the resulting CFCP prediction set obtained with the split-conformal threshold calibrated on D_q . Then*

$$\Pr\{Y_{n+1} \in \hat{\Gamma}(X_{n+1}) \mid \widehat{M}\} \geq 1 - \alpha.$$

Corollary 1 (Marginal validity). *Under the assumptions of Theorem 1,*

$$\Pr\{Y_{n+1} \in \hat{\Gamma}(X_{n+1})\} \geq 1 - \alpha.$$

Theorem 1 is the exact finite-sample guarantee for CFCP in the clean disjoint-split regime. Since CFCP uses sample-dependent soft mixtures over neighboring clusters rather than hard cluster-specific quantiles, we do not claim an exact clusterwise coverage theorem in general. Nevertheless, randomized APS admits a sharper oracle statement. If the final CFCP vector recovers the true conditional law, $q_x(c) = \Pr(Y = c \mid X = x)$, then the randomized APS true-label score is conditionally uniform given $X = x$, which yields exact local validity for any measurable region defined independently of the calibration labels.

Corollary 2 (Oracle local validity for randomized APS). *Assume the setting of Theorem 1, and suppose additionally that CFCP recovers the true conditional label law, i.e. $q_x(c) = \Pr(Y = c \mid X = x)$ for all x, c , and that the set constructor is randomized APS. Then for every measurable region $A \subseteq \mathcal{X}$ defined without using labels from D_q ,*

$$\Pr\{Y_{n+1} \in \hat{\Gamma}(X_{n+1}) \mid X_{n+1} \in A\} \geq 1 - \alpha.$$

A particularly relevant special case is the piecewise-constant cluster oracle: if clusters recover regions on which the conditional label distribution is constant and CFCP recovers this distribution, the same local-validity guarantee holds on each oracle cluster. See Corollary 3 in the appendix.

Oracle efficiency intuition. Beyond validity, CFCP also has a natural oracle efficiency intuition. Let $\mathcal{G}_{\text{glob}}$ denote the information available to a global predictor and let \mathcal{G}_{loc} denote the refined information obtained by augmenting it with the oracle neighborhood / cluster information used to construct q_x , with $\mathcal{G}_{\text{glob}} \subseteq \mathcal{G}_{\text{loc}}$, every $\mathcal{G}_{\text{glob}}$ -measurable set predictor is also \mathcal{G}_{loc} -measurable. Hence $\mathcal{A}(\mathcal{G}_{\text{glob}}, \alpha) \subseteq \mathcal{A}(\mathcal{G}_{\text{loc}}, \alpha)$. Define $V(\mathcal{G}, \alpha) = \inf_{\Gamma: \mathbb{P}(Y \in \Gamma(X) \mid \mathcal{G}) \geq 1 - \alpha} \mathbb{E}[|\Gamma(X)|]$. Since every global predictor is also admissible under the richer information set, it follows that $V(\mathcal{G}_{\text{loc}}, \alpha) \leq V(\mathcal{G}_{\text{glob}}, \alpha)$. Consequently, among predictors satisfying the same target coverage constraint, the expected set size of the population-optimal neighborhood-aware predictor is less than or equal to the population-optimal global predictor. Equivalently, at a fixed expected set-size budget, the best neighborhood-aware predictor attainable coverage is higher or equal. Define $U(\mathcal{G}, m) := \sup_{\Gamma: \Gamma(X) \text{ } \mathcal{G}\text{-measurable, } \mathbb{E}[|\Gamma(X)|] \leq m} \mathbb{P}(Y \in \Gamma(X))$. Then $U(\mathcal{G}_{\text{loc}}, m) \geq U(\mathcal{G}_{\text{glob}}, m)$.

This is a population-level motivation rather than a finite-sample dominance claim for CFCP because the practical method uses estimated cluster frequencies, reliability shrinkage and a single split-conformal threshold. Still, it explains why local cluster-frequency information improves efficiency in practice.

3.1 Computational complexity

CFCP is designed to scale to large embedding sets. Since the thresholding stage uses a standard split-conformal procedure such as LAC, APS, RAPS or SAPS, its computational overhead beyond ordinary conformal prediction is concentrated in the representation-space localization step, namely clustering and nearest-centroid retrieval. Complexity details are given in Appendix A.4.

4 Experiments

We evaluate CFCP through extensive experiments, comparing it with strong baselines across a diverse set of classification tasks and model architectures. Code for reproducing the experiments and is available at <https://anonymous.4open.science/r/CFCP-C039/>.

4.1 Experimental setup

This section describes the main components of the experimental setup. Full details on model training and experimental setup are available in Appendix C.1.

Datasets: We selected datasets in the many-class regime, where each class is supported by relatively few examples. CIFAR-100 (60,000 images, 100 classes) (Krizhevsky [2009]) and ImageNet ($\approx 1.33\text{M}$ images, 1000 classes, imbalanced) (Deng et al. [2009]) for image classification. ImageNet-V2 out-of-sample test set for ImageNet (10,000 images equally partitioned on the ImageNet classes) (Recht et al. [2019]). Web of Science (WOS-46985) ($\approx 47k$ records, 134 classes, imbalanced) (Kowsari et al. [2017]) for text classification.

Architectures: Fine-tuned ResNet-50 (He et al. [2016]) for CIFAR. Fine-tuned DistilBERT (Sanh et al. [2019]) on text data. For ImageNet we followed the training procedure of Ding et al. [2023], using SimCLR representations (Chen et al. [2020]) and a single layer prediction head.

Learned Representations: We follow Yosinski et al. [2014], Chen et al. [2020] to extract CNN activations and Transformer hidden states.

Baseline methods: We compared our CFCP method to Split, ICP, CCP, NCP and RC3P by evaluating each on these score methods: LAC, APS, RAPS and SAPS.

Coverage: $\alpha = 0.1$.

Uncertainty reporting: All reported result values are means with 95% CI over five repeated dataset splits with fixed seeds.

4.2 Evaluation metrics

Class Coverage: We report class coverage, defined as the number of classes whose empirical class-conditional coverage meets the target level $1 - \alpha$. Let $\widehat{\text{Cov}}_c$ denote the empirical class-conditional coverage for class c . We define Class Coverage at level α as $\widehat{\text{COV}} = \frac{1}{C} \sum_{c=1}^C \mathbf{1}\{\widehat{\text{Cov}}_c \geq 1 - \alpha\}$. This metric counts the number of classes whose empirical coverage meets the nominal target. Higher values are better, and $\widehat{\text{COV}} = 1$ iff all classes satisfy the target coverage level.

Efficiency (Set Size): We measure efficiency by the average set size, namely the mean number of labels contained in the prediction set across test examples. Let $\widehat{\Gamma}(x) \subseteq \{1, \dots, C\}$ denote the prediction set for input x . Its size is $|\widehat{\Gamma}(x)|$, the number of labels included in the set. Over a test set $\{(x_i, y_i)\}_{i=1}^n$, we define the empirical average set size as $\widehat{\text{Size}} = \frac{1}{n} \sum_{i=1}^n |\widehat{\Gamma}(x_i)| = \frac{1}{n} \sum_{i=1}^n \sum_{c=1}^C \mathbf{1}\{c \in \widehat{\Gamma}(x_i)\}$. Lower values for identical coverage level indicate greater efficiency.

Weighted under-coverage (WUC): Following the average class coverage gap (CovGap) definition (Ding et al. [2023]), we used its under-coverage variant (UnderCovGap) to evaluate the class conditional coverage. We preferred it over CovGap which penalizes methods which exhibit higher marginal coverage by considering over-coverage as an error. Let $\widehat{\text{Cov}}_c$ denote the empirical class-conditional coverage for class c , and let w_c be the empirical prevalence of class c in the test set, for $c = 1, \dots, C$ with $\sum_{c=1}^C w_c = 1$. We define the weighted under-coverage at level α as $\widehat{\text{WUC}}_p = \sum_{c=1}^C w_c \left[(1 - \alpha) - \widehat{\text{Cov}}_c \right]_+^p$, where $[u]_+ = \max(u, 0)$ and typically $p \in \{1, 2\}$, where $p = 1$ (used in our reports) gives a linear penalty and $p = 2$ penalizes severe under-coverage more strongly. This metric measures only coverage deficits relative to the target $1 - \alpha$, and equals zero iff all classes satisfy the nominal coverage target.

Max. coverage error (MaxCE): We report the maximum coverage error, which quantifies the worst under-covered class and therefore highlights whether gains in average classwise coverage mask severe failures on individual classes. Let $\widehat{\text{Cov}}_c$ denote the empirical class-conditional coverage for class c . We define the maximum coverage error at level α as $\widehat{\text{MaxCE}} = \max_{c \in \{1, \dots, C\}} \left[(1 - \alpha) - \widehat{\text{Cov}}_c \right]_+$, where $[u]_+ = \max(u, 0)$. This metric measures the worst classwise coverage shortfall relative to the nominal target. It is equal to zero iff all classes satisfy the target coverage level.

On our experiments we use $\widehat{\text{COV}}$ as primary metric and $\widehat{\text{Size}}$ as primary companion metric. Secondary diagnostics: $\widehat{\text{WUC}}$ and $\widehat{\text{MaxCE}}$. $\widehat{\text{COV}}$ is a natural binary version of the class-conditional coverage criterion. A closely related metric, Under Coverage Ratio (UCR), is used as the primary evaluation criterion in RC3P, and is equivalent to $1 - \widehat{\text{COV}}$. Ding et al. [2025] similarly report the fraction of classes with coverage below a threshold (FracBelow), showing that threshold-crossing counts and average-gap metrics are treated as complementary rather than competing.

4.3 Results

Table 1 reports within score-family comparisons at $\alpha = 0.1$. CFCP achieves the best class coverage in 15 of 16 dataset/score comparisons. The only exception is ImageNet-V2 with LAC, where Split is

Table 1: Within-family comparison of CFCP against baselines at $\alpha = 0.1$. Values are means over five repeated dataset splits. **Bold** marks the best class coverage within each family and, for set size, the lower value between CFCP and the best-coverage baseline. Full results including 95% CIs are in Appendix C.2.

Dataset	Score	CFCP (ours)		Split		ICP		CCP		NCP		RC3P	
		Cov \uparrow	Size \downarrow	Cov \uparrow	Size \downarrow	Cov \uparrow	Size \downarrow	Cov \uparrow	Size \downarrow	Cov \uparrow	Size \downarrow	Cov \uparrow	Size \downarrow
CIFAR-100	LAC	0.592	7.9	0.516	8.0	0.568	11.2	0.534	9.7	0.566	8.9	0.568	11.2
	APS	0.590	8.3	0.516	11.1	0.560	14.6	0.530	12.2	0.572	12.0	0.582	11.3
	RAPS	0.598	9.1	0.556	8.3	0.570	11.6	0.580	10.6	0.562	7.9	0.564	11.6
	SAPS	0.586	8.8	0.558	8.2	0.582	11.5	0.568	10.3	0.566	7.7	0.548	10.9
ImageNet	LAC	0.508	1.9	0.499	1.8	0.493	3.9	0.494	3.3	0.494	1.9	0.425	3.5
	APS	0.672	15.1	0.655	35.2	0.658	42.8	0.646	38.0	0.667	15.2	0.654	8.4
	RAPS	0.589	3.6	0.553	3.3	0.546	5.5	0.536	8.5	0.565	2.8	0.546	5.9
	SAPS	0.571	2.6	0.529	2.2	0.533	5.1	0.549	6.8	0.559	2.4	0.556	6.0
ImageNet-V2	LAC	0.446	2.5	0.452	2.4	0.388	5.0	0.386	4.3	0.445	2.8	0.424	6.9
	APS	0.714	31.2	0.710	64.7	0.708	72.0	0.707	69.2	0.704	39.8	0.712	28.1
	RAPS	0.552	4.8	0.525	4.3	0.523	6.4	0.529	8.8	0.541	4.2	0.544	10.2
	SAPS	0.465	3.0	0.458	2.8	0.463	5.5	0.455	7.4	0.446	2.8	0.440	6.0
WOS-46985	LAC	0.645	2.5	0.622	1.2	0.621	4.1	0.601	5.4	0.619	1.3	0.634	3.8
	APS	0.633	1.5	0.546	3.4	0.606	6.2	0.570	6.6	0.609	1.5	0.587	3.8
	RAPS	0.633	1.5	0.560	2.8	0.609	5.9	0.587	6.0	0.600	1.5	0.579	4.0
	SAPS	0.643	2.3	0.590	1.3	0.610	5.8	0.604	5.1	0.630	1.3	0.604	3.7

slightly better in class coverage. Overall, these results support the main goal of CFCP: improving the fraction of classes that satisfy the target coverage level while preserving the standard plug-in conformal set-construction framework.

The gains are consistent across modalities and score families. On CIFAR-100, ImageNet, and WOS-46985, CFCP obtains the best class coverage for all four score families. On ImageNet-V2, which is the hardest shifted test setting, CFCP obtains the best class coverage for APS, RAPS, and SAPS, and remains essentially tied with the best LAC baseline. These results suggest that local cluster-frequency information is useful not only for image classification, but also for text classification, and that the benefit is not tied to a particular conformal score.

The comparison with NCP is particularly informative because NCP is the closest local-neighborhood baseline and partly motivates CFCP. CFCP improves over NCP in class coverage in all 16 comparisons, supporting the methodological gap addressed here: locality alone, when implemented through point-wise neighborhood weighting of conformal scores, may be insufficient for classwise reliability. The advantage over NCP suggests that soft assignment to learned clusters, combined with global shrinkage when the local signal is unreliable, provides a more stable local signal than direct point-neighborhood weighting in high-dimensional many-class settings.

A second important finding is that CFCP’s class-coverage gains often come with strong efficiency. When comparing CFCP to the leading baseline in each dataset/score family, CFCP has the smaller average set size in 10 of 16 comparisons. Moreover, even when CFCP is not the smallest method, its set size is usually close to the most efficient competing baselines and often much smaller than the strongest class-coverage baseline. For example, on ImageNet with RAPS, CFCP improves class coverage from 0.565 for NCP and 0.546 for RC3P to 0.589, while keeping a small average set size of 3.6. Although NCP is smaller, CFCP substantially improves class coverage and remains more efficient than ICP, CCP and RC3P. On ImageNet-V2 with RAPS, CFCP achieves the best class coverage, 0.552, with a set size of 4.8, compared with 10.2 for RC3P, 6.4 for ICP, and 8.8 for CCP. It is only slightly larger than Split and NCP, which obtain lower class coverage. Thus, CFCP does not merely trade larger sets for higher class coverage. In many settings it improves class coverage while also producing competitive or more efficient prediction sets.

This observation is also consistent with recent findings that post-hoc temperature scaling can improve calibration while increasing the size of adaptive conformal prediction sets, since smoother probability vectors require APS/RAPS-style methods to accumulate more labels [Xi et al., 2024]. CFCP offers a

different route: when the local cluster signal is reliable, its probability vector is driven primarily by empirical cluster frequencies.

The secondary diagnostics in Appendix Table 4 reveal a more nuanced picture. CFCP is not uniformly best in weighted under-coverage or maximum coverage error. This is expected from the design of the method: CFCP uses soft mixtures of nearby cluster distributions together with a single global conformal threshold, so it improves broad classwise coverage but may still dilute rare or highly atypical classes. Consequently, CFCP can cover more classes overall while leaving a small number of hard classes with larger residual under-coverage. We therefore use WUC and MaxCE as diagnostics rather than primary selection criteria: they expose remaining tail failures, while class coverage and set size capture the main coverage-efficiency objective of the paper.

At the same time, the efficiency of CFCP gives the user room to operate at slightly higher marginal coverage when lower under-coverage is preferred. This is illustrated on ImageNet-V2, where increasing CFCP’s marginal coverage by 1% achieves the best WUC for both APS and RAPS while remaining markedly more efficient than the runner-up baselines. For APS, increasing marginal coverage by 1% yields WUC 0.041 with 0.737 COV and 35.8 Size, compared with 0.043, 0.71 and 64.7 for the strongest baseline. For RAPS, the corresponding values are 0.086, 0.574 and 5.2, versus 0.087, 0.529 and 8.8. This shows that CFCP’s efficiency advantage is not only a convenience, but also a practical degree of freedom for selecting a better coverage-efficiency operating point.

Finally, all methods require substantially larger prediction sets on ImageNet-V2 than on ImageNet, indicating that the distribution shift in ImageNet-V2 makes confident prediction more difficult. However, even in this harder regime, CFCP preserves its main qualitative advantage: it improves or matches the best class coverage while often maintaining a clear efficiency benefit.

Overall, Table 1 supports the main empirical claim. CFCP improves class coverage in nearly all within score-family comparisons and often achieves this improvement with equal or smaller prediction sets than the leading baseline. These results indicate that cluster-frequency information provides a useful localized signal for conformal prediction in many-class classification.

Sensitivity and ablation Our sensitivity analysis indicates that CFCP is task-adaptive rather than brittle. While the best hyperparameters depend on the dataset and model, reflecting differences in representation geometry and local label structure, our hyperparameter searches show that performance remains stable across a compact region of the hyperparameter space. In particular, near-best configurations typically differ by only about 1-2 percentage points in class coverage while maintaining closely matched set sizes, suggesting that CFCP’s improvements do not hinge on a single finely tuned setting but arise from the underlying local cluster-frequency mechanism itself. This is consistent with the role of CFCP’s locality-specific components: clustering granularity, neighborhood size, assignment temperature, smoothing and reliability-based shrinkage, which are designed to adapt the method to the structure of each task. Table 5 in the appendix shows a hyperparameter search example.

Ablations on ImageNet and ImageNet-V2 confirm that CFCP’s gains come from the combination of learned clusters and soft cluster assignment. Replacing the soft neighborhood mixture with hard nearest-cluster assignment generally reduces class coverage and substantially increases set size, especially for RAPS and SAPS. Conversely, removing clusters and relying only on a global label-frequency model collapses the locality mechanism: although it can recover moderate class coverage, it does so by producing very large prediction sets. These results support the role of soft cluster-frequency mixtures as the key component behind CFCP’s coverage-efficiency tradeoff. Full ablation results are reported in Table 6 in Appendix C.2.

In practice, the locality-specific hyperparameters can be selected on an internal validation split, with the final conformal threshold calibrated on a separate held-out calibration subset.

5 Discussion, limitations and future work

Our results indicate that local cluster-frequency information can improve conformal prediction by making prediction sets adapt to representation-space subpopulations rather than to a single global label distribution. CFCP improves class coverage while remaining competitive in set size, and in several settings substantially more efficient. More broadly, CFCP may help at the level of within-class

subpopulations when representation-space clusters capture meaningful local structure, though this remains a hypothesis beyond the experiments in this paper.

The main limitation is that smoothing across nearby clusters, together with a single global conformal threshold, can still dilute rare or atypical classes. As a result, CFCP may cover more classes overall while leaving a small number of hard classes with larger residual under-coverage or worse maximum coverage error. Appendix C.3 provides a CIFAR-100 failure-mode case study illustrating this behavior.

Future work should therefore focus on tail-sensitive extensions, such as class or cluster-aware threshold adjustments, adapting the framework to tabular problems using tree-ensemble representations, and generalizing the idea to conformal prediction for continuous labels via localized interval construction.

Acknowledgments and Disclosure of Funding

Use unnumbered first level headings for the acknowledgments. All acknowledgments go at the end of the paper before the list of references. Moreover, you are required to declare funding (financial activities supporting the submitted work) and competing interests (related financial activities outside the submitted work). More information about this disclosure can be found at: <https://neurips.cc/Conferences/2026/PaperInformation/FundingDisclosure>.

Do **not** include this section in the anonymized submission, only in the final paper. You can use the `ack` environment provided in the style file to automatically hide this section in the anonymized submission.

References

- Anastasios N Angelopoulos and Stephen Bates. A gentle introduction to conformal prediction and distribution-free uncertainty quantification. *arXiv preprint arXiv:2107.07511*, 2021.
- Ting Chen, Simon Kornblith, Kevin Swersky, Mohammad Norouzi, and Geoffrey E Hinton. Big self-supervised models are strong semi-supervised learners. *Advances in Neural Information Processing Systems*, 33:22243–22255, 2020. License: MIT.
- Jia Deng, Wei Dong, Richard Socher, Li-Jia Li, Kai Li, and Li Fei-Fei. Imagenet: A large-scale hierarchical image database. In *2009 IEEE conference on computer vision and pattern recognition*, pages 248–255. IEEE, 2009.
- Tiffany Ding, Anastasios N. Angelopoulos, Stephen Bates, Michael I. Jordan, and Ryan J. Tibshirani. Class-conditional conformal prediction with many classes. In *Advances in Neural Information Processing Systems*, 2023. URL <https://arxiv.org/abs/2306.09335>. NeurIPS 2023.
- Tiffany Ding, Jean-Baptiste Fermanian, and Joseph Salmon. Conformal prediction for long-tailed classification. *arXiv preprint arXiv:2507.06867*, 2025.
- Matthijs Douze, Alexandr Guzhva, Chengqi Deng, Jeff Johnson, Gergely Szilvasy, Pierre-Emmanuel Mazaré, Maria Lomeli, Lucas Hosseini, and Hervé Jégou. The faiss library. *IEEE Transactions on Big Data*, 2025. License: MIT.
- Subhankar Ghosh, Taha Belkhouja, Yan Yan, and Janardhan Rao Doppa. Improving uncertainty quantification of deep classifiers via neighborhood conformal prediction: Novel algorithm and theoretical analysis. In *Proceedings of the AAAI Conference on Artificial Intelligence*, volume 37, pages 7722–7730, 2023. doi: 10.1609/aaai.v37i6.25936. URL <https://ojs.aaai.org/index.php/AAAI/article/view/25936>.
- Natalia Martinez Gil, Dhaval Patel, Chandra Reddy, Giri Ganapavarapu, Roman Vaculin, and Jayant Kalagnanam. Identifying homogeneous and interpretable groups for conformal prediction. In *Uncertainty in Artificial Intelligence*, pages 2471–2485. PMLR, 2024.
- Kaiming He, Xiangyu Zhang, Shaoqing Ren, and Jian Sun. Deep residual learning for image recognition. In *Proceedings of the IEEE conference on computer vision and pattern recognition*, pages 770–778, 2016. License: BSD.
- Rohan Hore and Rina Foygel Barber. Conformal prediction with local weights: Randomization enables local guarantees. *arXiv preprint arXiv:2310.07850*, 2023. URL <https://arxiv.org/abs/2310.07850>.
- Jianguo Huang, Huajun Xi, Linjun Zhang, Huaxiu Yao, Yue Qiu, and Hongxin Wei. Conformal prediction for deep classifier via label ranking. *arXiv preprint arXiv:2310.06430*, 2023.
- Jianguo Huang, Jianqing Song, Xuanning Zhou, Bingyi Jing, and Hongxin Wei. Torchcp: A python library for conformal prediction, 2024. License: GNU GPL, LGPL.
- Kamran Kowsari, Donald E Brown, Mojtaba Heidarysafa, Kiana Jafari Meimandi, Matthew S Gerber, and Laura E Barnes. Hdltext: Hierarchical deep learning for text classification. In *2017 16th IEEE international conference on machine learning and applications (ICMLA)*, pages 364–371. IEEE, 2017. License: CC-BY 4.0.
- Alex Krizhevsky. Learning multiple layers of features from tiny images. Technical report, University of Toronto, 2009. License: CC-BY 4.0.
- Adam Paszke, Sam Gross, Francisco Massa, Adam Lerer, James Bradbury, Gregory Chanan, Trevor Killeen, Zeming Lin, Natalia Gimelshein, Luca Antiga, et al. Pytorch: An imperative style, high-performance deep learning library. *Advances in Neural Information Processing Systems*, 32, 2019. License: BSD.
- Benjamin Recht, Rebecca Roelofs, Ludwig Schmidt, and Vaishaal Shankar. Do imagenet classifiers generalize to imagenet? In *International conference on machine learning*, pages 5389–5400. PMLR, 2019. License: MIT.

- Yaniv Romano, Matteo Sesia, and Emmanuel Candes. Classification with valid and adaptive coverage. *Advances in Neural Information Processing Systems*, 33:3581–3591, 2020.
- Mauricio Sadinle, Jing Lei, and Larry Wasserman. Least ambiguous set-valued classifiers with bounded error levels. *Journal of the American Statistical Association*, 114(525):223–234, 2019.
- Victor Sanh, Lysandre Debut, Julien Chaumond, and Thomas Wolf. Distilbert, a distilled version of bert: smaller, faster, cheaper and lighter. *arXiv preprint arXiv:1910.01108*, 2019. License: Apache.
- Yuanjie Shi, Subhankar Ghosh, Taha Belkhouja, Janardhan R Doppa, and Yan Yan. Conformal prediction for class-wise coverage via augmented label rank calibration. *Advances in Neural Information Processing Systems*, 37, 2024.
- Vladimir Vovk. Conditional validity of inductive conformal predictors. In Steven C. H. Hoi and Wray Buntine, editors, *Proceedings of the Asian Conference on Machine Learning*, volume 25 of *Proceedings of Machine Learning Research*, pages 475–490, Singapore, 2012. PMLR. URL <https://proceedings.mlr.press/v25/vovk12.html>.
- Vladimir Vovk, Alexander Gammerman, and Glenn Shafer. *Algorithmic learning in a random world*. Springer, 2005.
- Huajun Xi, Jianguo Huang, Kangdao Liu, Lei Feng, and Hongxin Wei. Does confidence calibration improve conformal prediction? *arXiv preprint arXiv:2402.04344*, 2024.
- Jason Yosinski, Jeff Clune, Yoshua Bengio, and Hod Lipson. How transferable are features in deep neural networks? *Advances in Neural Information Processing Systems*, 27, 2014.
- Yao Zhang and Emmanuel J. Candès. Posterior conformal prediction. *arXiv preprint arXiv:2409.19712*, 2024. URL <https://arxiv.org/abs/2409.19712>.

A Additional Method Details

Table 2: Notation used in the CFCP method.

Symbol	Type	Definition
$x \in \mathcal{X}$	input	Input example.
$y, c \in \mathcal{Y}$	label	True label y or candidate class c .
C	scalar	Number of classes, $ \mathcal{Y} = C$.
f	model	Pre-trained classifier.
$\phi(x) \in \mathbb{R}^d$	vector	Learned representation of x .
z	vector	ℓ_2 -normalized embedding of x .
d	scalar	Embedding dimension.
K	scalar	Number of representation-space clusters.
$\mu_k \in \mathbb{R}^d$	vector	Centroid of cluster k , for $k = 1, \dots, K$.
m	scalar	Number of nearest centroids used for soft assignment.
$\kappa_j(x)$	index	Index of the j -th nearest centroid to x .
$\delta_j(x)$	scalar	Cosine similarity between z and centroid $\mu_{\kappa_j(x)}$.
$w_j(x)$	scalar	Soft assignment weight of x to its j -th nearest centroid.
τ	scalar	Softmax temperature controlling assignment sharpness. Smaller values yield more local assignments.
$\mathcal{D}_{\text{stat}}$	set	Calibration subset used to estimate cluster-level label statistics.
\mathcal{D}_q	set	Held-out calibration subset used to estimate the conformal threshold.
N_{kc}	scalar	Soft count of calibration samples from class c assigned to cluster k .
S_k	scalar	Effective support of cluster k , i.e., total soft mass assigned to cluster k .
$\pi \in \Delta^{C-1}$	vector	Global prior used for smoothing cluster label distributions.
β	scalar	Dirichlet smoothing strength toward π .
$\hat{p}_k(c)$	scalar	Smoothed empirical probability of class c in cluster k .
$q_x^{\text{local}}(c)$	scalar	Local cluster-frequency mixture probability for class c at test point x .
$\pi_x(c)$	scalar	Fallback prior for class c at x , e.g., the base model probability.
γ	scalar	Exponent controlling the effect of assignment concentration in the reliability score.
β_{sup}	scalar	Support-shrinkage parameter controlling the effect of neighborhood support.
$r(x) \in [0, 1]$	scalar	Reliability weight used to interpolate between local cluster frequencies and the fallback prior.
$q_x(c)$	scalar	Final CFCP probability assigned to class c for input x .
$s(x, c)$	scalar	Nonconformity score of candidate class c for input x .
α	scalar	Target miscoverage level.
$\hat{q}_{1-\alpha}$	scalar	Split-conformal quantile calibrated on \mathcal{D}_q .
$\hat{\Gamma}(x)$	set	Conformal prediction set returned for input x .

A.1 CFCP score construction details

CFCP builds a sample-specific class-probability vector from local cluster-frequency information in a learned representation space. Let $\phi(x) \in \mathbb{R}^d$ denote the representation of input x , and let all embeddings and centroids be ℓ_2 -normalized. After fitting spherical k -means on the training representations, we obtain centroids μ_1, \dots, μ_K .

For a point x with normalized embedding z , we retrieve its top- m nearest centroids $c_1(x), \dots, c_m(x)$ with cosine similarities $\delta_1(x), \dots, \delta_m(x)$. These similarities are converted into soft assignment weights

$$w_j(x) = \frac{\exp(\delta_j(x)/\tau)}{\sum_{\ell=1}^m \exp(\delta_\ell(x)/\tau)}, \quad j = 1, \dots, m, \quad (7)$$

where $\tau > 0$ controls the sharpness of the local assignment. Lower values yield more local assignments.

Let D_{stat} denote the calibration subset used to estimate local label statistics. Each calibration point contributes fractionally to its neighboring clusters. The resulting soft cluster-label counts and effective supports are

$$N_{kc} = \sum_{(x_i, y_i) \in D_{\text{stat}}} \sum_{j=1}^m w_{ij} \mathbf{1}\{k_j(x_i) = k, y_i = c\}, \quad (8)$$

$$S_k = \sum_{(x_i, y_i) \in D_{\text{stat}}} \sum_{j=1}^m w_{ij} \mathbf{1}\{k_j(x_i) = k\}. \quad (9)$$

We then estimate a smoothed cluster-level label distribution

$$\hat{p}_k(c) = \frac{N_{kc} + \beta \pi_c}{S_k + \beta}, \quad c = 1, \dots, C, \quad (10)$$

where $\beta > 0$ is a smoothing parameter and $\pi \in \Delta^{C-1}$ is a global prior. In our implementation, π can be taken either as the empirical label prior or as the mean of the base model’s class-probability vectors on D_{stat} .

For a test point x , the local cluster-frequency mixture is

$$q_x^{\text{local}}(c) = \sum_{j=1}^m w_j(x) \hat{p}_{k_j(x)}(c), \quad c = 1, \dots, C. \quad (11)$$

This vector serves as the local probabilistic summary of the representation-space neighborhood of x .

A.2 Reliability shrinkage details

The local mixture q_x^{local} may be unstable when a point lies between several centroids or when its neighboring clusters have little support in calibration. CFCP therefore applies reliability-aware shrinkage toward a fallback prior π_x .

We first define assignment concentration by

$$\text{conf}(x) = \left(\max_{1 \leq j \leq m} w_j(x) \right)^\gamma, \quad (12)$$

where $\gamma > 0$ controls how strongly the method rewards concentrated local assignments. Next, we define neighborhood support as the weighted average support of the neighboring clusters,

$$\text{sup}(x) = \sum_{j=1}^m w_j(x) S_{k_j(x)}, \quad (13)$$

and convert it into a normalized support weight,

$$\text{supw}(x) = \frac{\text{sup}(x)}{\text{sup}(x) + \beta_{\text{sup}}}, \quad (14)$$

where $\beta_{\text{sup}} > 0$ regularizes the effect of local support.

The resulting reliability score is

$$r(x) = \text{conf}(x) \text{supw}(x) \in [0, 1]. \quad (15)$$

Finally, CFCP interpolates between the local cluster-frequency mixture and the fallback prior:

$$q_x(c) = r(x) q_x^{\text{local}}(c) + (1 - r(x)) \pi_x(c), \quad c = 1, \dots, C. \quad (16)$$

Reliability shrinkage therefore serves two roles: it preserves locality when the cluster signal is strong and it prevents unstable local estimates from dominating when the neighborhood is ambiguous or weakly supported.

A.3 LAC/APS/RAPS/SAPS instantiations

After constructing q_x , CFCP applies a standard split-conformal set constructor. Let $D_q = \{(x_i, y_i)\}_{i=1}^{n_q}$ denote the calibration subset used only for quantile estimation. Given a nonconformity score $s(x, y)$ induced by the chosen constructor, we compute

$$S_i = s(x_i, y_i), \quad i = 1, \dots, n_q, \quad (17)$$

and set the split-conformal threshold

$$\hat{q}_{1-\alpha} = S_{(k)}, \quad k = \lceil (n_q + 1)(1 - \alpha) \rceil, \quad (18)$$

where $S_{(k)}$ is the k -th order statistic.

LAC. For the LAC-style instantiation, the nonconformity score is

$$s_{\text{LAC}}(x, y) = 1 - q_x(y). \quad (19)$$

The resulting prediction set is

$$\hat{\Gamma}_{\text{LAC}}(x) = \{c \in \{1, \dots, C\} : q_x(c) \geq 1 - \hat{q}_{1-\alpha}\}. \quad (20)$$

In implementation, we enforce non-emptiness by including the top-ranked label when needed.

APS. Let $\pi_x^{(1)}, \dots, \pi_x^{(C)}$ denote the labels sorted in decreasing order of $q_x(c)$, and let

$$Q_x^{(j)} = q_x(\pi_x^{(j)}). \quad (21)$$

If the true label y appears at rank $r_x(y)$, the deterministic APS score is

$$s_{\text{APS}}(x, y) = \sum_{j=1}^{r_x(y)} Q_x^{(j)}. \quad (22)$$

Under randomized APS, the score becomes

$$s_{\text{APS}}^{\text{rand}}(x, y) = \sum_{j=1}^{r_x(y)-1} Q_x^{(j)} + U_x Q_x^{(r_x(y))}, \quad U_x \sim \text{Unif}(0, 1). \quad (23)$$

The APS prediction set is the smallest top-probability prefix whose cumulative score does not exceed $\hat{q}_{1-\alpha}$.

RAPS. RAPS augments APS with rank-dependent regularization. Let $\lambda \geq 0$ be the regularization strength and $k_{\text{reg}} \in \mathbb{N}$ the un-penalized rank. The deterministic RAPS score is

$$s_{\text{RAPS}}(x, y) = s_{\text{APS}}(x, y) + \lambda \max\{0, r_x(y) - k_{\text{reg}}\}, \quad (24)$$

and the randomized variant replaces $s_{\text{APS}}(x, y)$ by $s_{\text{APS}}^{\text{rand}}(x, y)$. As in APS, the prediction set is the smallest prefix of the labels sorted by $q_x(c)$ whose adjusted cumulative score remains below $\hat{q}_{1-\alpha}$, with a top-1 fallback to avoid empty sets.

SAPS. Sorted Adaptive Prediction Sets (SAPS) is a rank-based alternative that depends on the ordering induced by q_x rather than on its full cumulative mass. Let $\pi_x^{(1)}, \dots, \pi_x^{(C)}$ be the labels sorted in decreasing order of $q_x(c)$, and let $p_{(1)}(x) = q_x(\pi_x^{(1)})$ denote the top-1 probability. For a label at rank $r_x(y) \in \{0, \dots, C-1\}$, SAPS assigns the score

$$s_{\text{SAPS}}(x, y) = p_{(1)}(x) + w r_x(y), \quad (25)$$

where $w > 0$ is a constant rank increment. In the randomized variant, the score is

$$s_{\text{SAPS}}^{\text{rand}}(x, y) = p_{(1)}(x) + w r_x(y) - U_x w, \quad U_x \sim \text{Unif}(0, 1), \quad (26)$$

with the rank-1 label using $p_{(1)}(x) - U_x p_{(1)}(x)$ instead. Thus SAPS constructs prediction sets by traversing the labels sorted by q_x and adding a fixed penalty per lower rank, yielding a simpler rank-sensitive alternative to APS and RAPS. In CFDP, SAPS is applied in the same plug-in manner as the other set constructors, with the ranking determined by the local cluster-frequency probability vector q_x .

These instantiations make clear that CFDP is a plug-in conformal framework: the conformal score and thresholding rules are standard, and the only CFDP-specific component is the local construction of the probability vector q_x from cluster-frequency information.

A.4 Computational complexity

CFDP is designed to scale to large embedding sets. Since the thresholding stage uses a standard split-conformal procedure such as LAC, APS, RAPS or SAPS, its computational overhead beyond ordinary conformal prediction is concentrated in the representation-space localization step, namely clustering and nearest-centroid retrieval. Training requires clustering only the training embeddings into K centroids. At test time, inference compares each point against centroids rather than against all training examples, reducing the locality search to a top- m nearest-centroid lookup. In practice, we implement both spherical k -means and nearest-centroid retrieval using FAISS (Douze et al. [2025]), and we process examples in chunks to control memory use.

Let n_{train} be the number of training embeddings, d the embedding dimension, K the number of clusters, T the number of spherical k -means iterations and n the number of points to score at inference or calibration time. A standard spherical k -means pass requires assigning each embedding to its nearest centroid and recomputing centroids, yielding time complexity $O(T n_{\text{train}} K d)$. After clustering, FAISS nearest-centroid retrieval with a flat inner-product index over normalized centroids requires $O(K d)$ work per query, hence $O(n K d)$ over n queries, after which only the top- m neighbors are retained. The remaining conformal thresholding and set-construction steps use the same order of computation as their standard split-conformal counterparts, applied to the probability vectors q_x .

Compared with point-wise neighborhood methods, this centroid-based design offers a favorable tradeoff between locality and scalability: the method remains representation-aware and locally adaptive, while avoiding full nearest-neighbor search over all embedded training samples.

B Validity proofs

This appendix formalizes the validity claims for CFDP in the disjoint-split regime. The proof strategy separates the standard split-conformal marginal guarantee from a stronger oracle local statement that is specific to randomized APS. The latter is inspired by the randomized oracle construction of Romano et al. [2020]. Our theorem is a new specialization of that idea to the case where CFDP recovers the true conditional label law. The broader oracle perspective is also aligned with Sadinle et al. [2019], while the need for additional assumptions in local validity is consistent with the conditional-validity literature [Vovk, 2012, Hore and Barber, 2023].

B.1 Exact marginal validity

B.1.1 Proof of Theorem 1.

Let \widehat{M} denote all quantities fitted before quantile calibration, including the representation map, centroids, soft cluster statistics, smoothed cluster distributions, reliability terms, and any fallback prior used to form q_x . Assume that:

1. $D_{\text{train}}, D_{\text{stat}}, D_q$, and the test point (X_{n+1}, Y_{n+1}) are mutually disjoint, and $\{(X_i, Y_i) : i \in D_q\} \cup \{(X_{n+1}, Y_{n+1})\}$ are exchangeable.
2. \widehat{M} is constructed without using labels from D_q .
3. Any auxiliary probabilities used in the fallback prior for points in D_q and at test time are produced without using labels from D_q .
4. If randomized APS or randomized RAPS is used, the auxiliary random variables are i.i.d. and independent of the data.

Define the calibration scores

$$S_i = s(X_i, Y_i), \quad (X_i, Y_i) \in D_q,$$

and let

$$\widehat{q}_{1-\alpha} = S_{(k)}, \quad k = \lceil (|D_q| + 1)(1 - \alpha) \rceil,$$

where $S_{(k)}$ is the k th order statistic. Then, conditional on \widehat{M} ,

$$\Pr\{Y_{n+1} \in \widehat{\Gamma}(X_{n+1}) \mid \widehat{M}\} \geq 1 - \alpha.$$

Proof. Conditional on \widehat{M} , the score map $(x, y) \mapsto s(x, y)$ is fixed. By Assumptions 1-4, the calibration scores $\{S_i : (X_i, Y_i) \in D_q\}$ and the test score $S_{n+1} = s(X_{n+1}, Y_{n+1})$ are exchangeable conditional on \widehat{M} . Standard split conformal rank arguments therefore imply

$$\Pr\{S_{n+1} \leq \widehat{q}_{1-\alpha} \mid \widehat{M}\} \geq 1 - \alpha.$$

By construction, $S_{n+1} \leq \widehat{q}_{1-\alpha}$ implies $Y_{n+1} \in \widehat{\Gamma}(X_{n+1})$. Any non-empty-set fallback can only enlarge the prediction set and therefore preserves the coverage lower bound. Hence

$$\Pr\{Y_{n+1} \in \widehat{\Gamma}(X_{n+1}) \mid \widehat{M}\} \geq 1 - \alpha.$$

□

B.1.2 Proof of Corollary 1

Under the assumptions of Theorem 1,

$$\Pr\{Y_{n+1} \in \widehat{\Gamma}(X_{n+1})\} \geq 1 - \alpha.$$

Proof. Take expectations in Theorem 1 with respect to \widehat{M} . □

B.2 Proof of Corollary 2

The next result is specific to randomized APS. Its intuition comes from the oracle randomized classifier of Romano et al. [2020]: if the predictive probability vector equals the true conditional label law, then the randomized cumulative-probability score acts as a discrete probability integral transform.

Lemma 2 (Conditional uniformity of the randomized APS score). *Fix $x \in \mathcal{X}$, and suppose $q_x(c) = \eta_c(x) := \Pr(Y = c \mid X = x)$ for all $c \in \{1, \dots, C\}$. Let $\pi_x^{(1)}, \dots, \pi_x^{(C)}$ be the labels sorted in decreasing order of $q_x(c)$, and let $Q_x^{(j)} = q_x(\pi_x^{(j)})$. If $Y \sim \eta(\cdot \mid x)$ and $U \sim \text{Unif}(0, 1)$ is independent, define*

$$S^{\text{randAPS}}(x, Y, U) = \sum_{j=1}^{r_x(Y)-1} Q_x^{(j)} + U Q_x^{(r_x(Y))},$$

where $r_x(Y)$ is the rank of Y in the ordering induced by q_x . Then

$$S^{\text{randAPS}}(x, Y, U) \mid X = x \sim \text{Unif}(0, 1).$$

Proof. For a fixed x , the sorted probabilities partition $[0, 1]$ into intervals. Let:

$$B_j(x) = \sum_{\ell < j} Q_x^{(\ell)}, \quad j = 1, \dots, C,$$

and define

$$I_j(x) = [B_j(x), B_j(x) + Q_x^{(j)}), \quad j < C,$$

with the last interval closed on the right. Then the intervals partition $[0, 1]$ and $|I_j(x)| = Q_x^{(j)}$.

Under $Y \sim \eta(\cdot | x) = q_x$, label $\pi_x^{(j)}$ is selected with probability $Q_x^{(j)}$. Conditional on selecting that label, the randomized score $S^{\text{randAPS}}(x, Y, U)$ is uniform on $I_j(x)$. Therefore, conditional on $X = x$, the random variable $S^{\text{randAPS}}(x, Y, U)$ is a mixture of uniforms on the intervals $I_j(x)$ with weights equal to the interval lengths $|I_j(x)| = Q_x^{(j)}$, and hence

$$S^{\text{randAPS}}(x, Y, U) | X = x \sim \text{Unif}(0, 1).$$

□

Theorem 3 (Oracle local validity of disjoint-split CFCP with randomized APS). *Assume the setting of Theorem 1. In addition, assume:*

1. **Oracle recovery:**

$$q_x(c) = \eta_c(x) := \Pr(Y = c | X = x), \quad \forall x, c.$$

2. **Randomized APS score:** CFCP uses randomized APS, i.e.

$$S^{\text{randAPS}}(x, y; u) = \sum_{j=1}^{r_x(y)-1} Q_x^{(j)} + u Q_x^{(r_x(y))}, \quad u \sim \text{Unif}(0, 1),$$

with independent randomization and a fixed tie-breaking rule.

Let $\hat{q}_{1-\alpha}$ be the split-conformal quantile computed on D_q , and let $\hat{\Gamma}$ be the resulting randomized APS prediction set. Then for every measurable region $A \subseteq \mathcal{X}$ defined without using labels from D_q ,

$$\Pr\{Y_{n+1} \in \hat{\Gamma}(X_{n+1}) | X_{n+1} \in A\} \geq 1 - \alpha.$$

Proof. By Lemma 2, for every fixed x ,

$$S_{n+1} := S^{\text{randAPS}}(X_{n+1}, Y_{n+1}; U_{n+1}) | X_{n+1} = x \sim \text{Unif}(0, 1).$$

Hence for every measurable region A ,

$$S_{n+1} | \{X_{n+1} \in A\} \sim \text{Unif}(0, 1).$$

The same is true for the calibration scores in D_q , since the oracle assumption holds for all calibration points as well. Because A is defined independently of the labels in D_q , conditioning on $X_{n+1} \in A$ does not disturb the exchangeability of the calibration scores and the test score conditional on \widehat{M} . Therefore, the split-conformal rank argument applies conditionally on $\{X_{n+1} \in A\}$:

$$\Pr\{S_{n+1} \leq \hat{q}_{1-\alpha} | X_{n+1} \in A\} \geq 1 - \alpha.$$

Finally, by the definition of randomized APS,

$$Y_{n+1} \in \hat{\Gamma}(X_{n+1}) \iff S_{n+1} \leq \hat{q}_{1-\alpha},$$

which proves the claim. □

Corollary 3 (Piecewise-constant cluster oracle). *Assume there exists a measurable partition*

$$\mathcal{X} = A_1 \cup \dots \cup A_K$$

such that for each k there is a probability vector $p_k \in \Delta^{C-1}$ satisfying

$$\Pr(Y = c | X = x) = p_k(c), \quad \forall x \in A_k, \forall c.$$

Assume further that CFCP recovers this oracle structure in the sense that for every $x \in A_k$,

$$q_x = p_k.$$

Then the conclusion of Theorem 3 holds on every cluster A_k :

$$\Pr\{Y_{n+1} \in \hat{\Gamma}(X_{n+1}) | X_{n+1} \in A_k\} \geq 1 - \alpha, \quad k = 1, \dots, K.$$

Proof. Apply Theorem 3 with $A = A_k$. □

Remark: (Why this theorem is specific to randomized APS) Theorem 3 relies on the conditional uniformity in Lemma 2. This property is natural for randomized APS, but it does not hold in general for the LAC score $1 - q_x(y)$, deterministic APS, RAPS or SAPS. Therefore we do not claim exact local validity for the full CFCP score-family. Outside randomized APS, local validity should be understood through approximate score-homogenization statements.

B.3 Approximate local validity

The next proposition formalizes the general intuition of CFCP: if the local score distribution within a region A is close to the global score distribution used for calibration, then the local coverage error in A is small.

Proposition 1 (Approximate local validity from score homogenization). *Assume the setting of Theorem 1, and let*

$$S = s(X, Y; U)$$

denote the nonconformity score of a fresh point under any supported CFCP set constructor. Let

$$F(t) = \Pr(S \leq t), \quad F_A(t) = \Pr(S \leq t \mid X \in A)$$

be the global and local score distribution functions, respectively, for a measurable region $A \subseteq \mathcal{X}$. Let

$$q_{1-\alpha}^* = \inf\{t : F(t) \geq 1 - \alpha\}.$$

If

$$\sup_t |F_A(t) - F(t)| \leq \varepsilon_A$$

for some $\varepsilon_A \geq 0$, then the population-thresholded prediction set

$$\Gamma^*(x) = \{c : s(x, c; U) \leq q_{1-\alpha}^*\}$$

satisfies

$$\Pr\{Y_{n+1} \in \Gamma^*(X_{n+1}) \mid X_{n+1} \in A\} \geq 1 - \alpha - \varepsilon_A.$$

Proof. By definition of $q_{1-\alpha}^*$,

$$F(q_{1-\alpha}^*) \geq 1 - \alpha.$$

Therefore

$$F_A(q_{1-\alpha}^*) \geq F(q_{1-\alpha}^*) - \sup_t |F_A(t) - F(t)| \geq 1 - \alpha - \varepsilon_A.$$

Since

$$\{Y_{n+1} \in \Gamma^*(X_{n+1})\} = \{S_{n+1} \leq q_{1-\alpha}^*\},$$

the result follows. \square

Remark (Connection to the finite-sample CFCP procedure) Proposition 1 is stated at the population quantile $q_{1-\alpha}^*$ to isolate the local-homogenization effect. In the actual split-conformal procedure, $q_{1-\alpha}^*$ is replaced by the empirical order-statistic threshold $\hat{q}_{1-\alpha}$. The resulting set inherits the same qualitative conclusion, up to the usual finite-sample rank-calibration conservatism already captured by Theorem 1.

C Experiments and results

C.1 Experimental setup

C.1.1 Data sets and models

- **CIFAR-100** (Krizhevsky [2009]): we followed the training procedure from Ding et al. [2023].
 - Splits: The datasets include 50,000 train images and 10,000 test images equally distributed over 10/100 classes. We split the training data to 60% and 40% validation. The test data was split to five repeated holdouts with fixed seeds to 75% calibration, and 25% testing.

- Model: PyTorch (Paszke et al. [2019]) ResNet-50 (He et al. [2016]), initialized to the IMAGENET1K_V2 (Deng et al. [2009]) weights and then fine-tuned all parameters for 30 epochs. Validation accuracy is 60%.
- **ImageNet** (Deng et al. [2009]): we followed the training procedure from Ding et al. [2023].
 - Splits: We sampled random 100,000 images of the $\approx 1M$ training set for training and another five repeated holdouts with fixed seeds of 100,000 images for conformal prediction calibration and validation. We used the 50,000 ImageNet’s validation set for testing. In addition, we used ImageNet-V2’s test set using the classification and conformal prediction models of ImageNet’s experiment.
 - Model: Based on a SimCLR-v2 model (Chen et al. [2020]), which was trained on the ImageNet training set without labels, to extract feature vectors of length 6,144 for all images in the ImageNet training set, we trained a classifier using one fully connected prediction head. Validation accuracy is 78%.
- **WOS-46985**: We used the keywords and abstract texts to train a classification model on the dataset.
 - Splits: 70% of the data were randomly sampled for training. The remaining 30% were split to five repeated holdouts with fixed seeds to 65% conformal prediction calibration and 35% testing.
 - Model: We used DistilBERT (Sanh et al. [2019]) classifier fine-tuned with num_train_epochs=5, learning_rate=2e-5, weight_decay=0.01, warmup_ratio=0.1. Validation accuracy is 88.4%.
- **Baseline methods**: We compared our CFCP method to Split, ICP, CCP, NCP and RC3P by evaluating each on these score methods: LAC, APS, RAPS and SAPS. For the Split, ICP and CCP, baseline methods and all scores implementation we used the TorchCP framework (Huang et al. [2024]). For the NCP and RC3P baselines we repeated the implementation that was shared by the authors in the original papers.
- **Method parameters**:
 - Score: We used equal parameters for scoring on both CFCP and baseline methods. APS/RAPS/SAPS: randomized=True, RAPS: penalty=0.1, kreg=5 for CIFAR-100 and WOS-46985, 20 for ImageNet, SAPS: weight=0.2.
 - Prediction set construction: We used temperature=1 for all methods.
 - CCP: ratio_clustering="auto", num_clusters="auto".
 - NCP: localizer tuned using "logits" from the authors’ implementation and "features" as mentioned in the original paper (we used CNN activations and Transformer hidden states), use_platt_scaling=True, k tuned using grid {0.05, 0.10, 0.20, 0.40}, lambda_L tuned using grid {10, 50, 100, 500, 1000, 5000}, hyper_fraction=0.3.
 - RC3P: variant = 'mix', mix_grid_size=50, hyper_fraction=0, coverage_slack=0.
 - CFCP locality-specific hyperparameters were tuned per dataset: n_clusters (K), n_neighbors (m), cluster assignment τ , Dirichlet smoothing (β), reliability gamma (γ), reliability beta support (β_{sup}). These hyperparameters were selected on an internal tuning split from the calibration pool.
- **Calibration sub-splits**: We tuned locality-specific hyperparameters per dataset: $n_{\text{clusters}}(K)$, $n_{\text{neighbors}}(m)$, cluster-assignment temperature τ , Dirichlet smoothing β , reliability gamma γ , and reliability beta support β_{sup} . For each outer data split, we partitioned the non-test conformal pool into D_{stat} , D_{tune} , D_q with proportions (0.6/0.2/0.2). D_{stat} was used to estimate the local cluster-frequency model, D_{tune} was used only for hyperparameter selection via an internal split into quantile-calibration and evaluation subsets, and D_q was reserved exclusively for the final conformal quantile. After hyperparameter selection, we refit the CFCP local model on $D_{\text{stat}} \cup D_{\text{tune}}$ and calibrated the final conformal threshold on the untouched D_q . Baseline methods were calibrated on the same calibration pool and all methods were evaluated on the same untouched test set.

C.1.2 Compute

All experiments were performed on a Macbook Pro M4 Max 36GB RAM. A full run of all reported CFCP experiments required approximately 3-4 hours. Individual dataset runs required approximately 30-60 minutes depending on the dataset.

C.2 Additional results

Table 3: Full results. Each metric column reports mean \pm 95 % CI over five repeated splits. **Bold** marks the best class coverage within each (Dataset / Score) group.

Score	Method	Class Cov. (\uparrow)	Set Size (\downarrow)	WUC (\downarrow)	MaxCE (\downarrow)
CIFAR-100					
LAC	CFCP	0.592 \pm 0.057	7.9 \pm 0.4	0.030 \pm 0.009	0.196 \pm 0.027
	RC3P	0.568 \pm 0.042	11.2 \pm 0.5	0.026 \pm 0.005	0.164 \pm 0.027
	ICP	0.568 \pm 0.042	11.2 \pm 0.5	0.026 \pm 0.005	0.164 \pm 0.027
	Split	0.516 \pm 0.034	8.0 \pm 0.2	0.033 \pm 0.006	0.228 \pm 0.042
	NCP	0.566 \pm 0.056	8.9 \pm 0.5	0.023 \pm 0.005	0.164 \pm 0.044
	CCP	0.534 \pm 0.069	9.7 \pm 0.5	0.027 \pm 0.007	0.204 \pm 0.027
APS	CFCP	0.590 \pm 0.039	8.3 \pm 0.5	0.025 \pm 0.009	0.220 \pm 0.070
	RC3P	0.582 \pm 0.032	11.3 \pm 0.1	0.025 \pm 0.002	0.196 \pm 0.057
	ICP	0.560 \pm 0.046	14.6 \pm 0.6	0.026 \pm 0.005	0.188 \pm 0.022
	Split	0.516 \pm 0.045	11.1 \pm 0.3	0.032 \pm 0.006	0.212 \pm 0.022
	NCP	0.572 \pm 0.039	12.0 \pm 0.5	0.024 \pm 0.005	0.172 \pm 0.022
	CCP	0.530 \pm 0.066	12.2 \pm 1.0	0.029 \pm 0.009	0.188 \pm 0.022
RAPS	CFCP	0.598 \pm 0.034	9.1 \pm 0.6	0.031 \pm 0.007	0.212 \pm 0.042
	RC3P	0.564 \pm 0.037	11.6 \pm 0.2	0.025 \pm 0.003	0.172 \pm 0.042
	ICP	0.570 \pm 0.041	11.6 \pm 0.2	0.025 \pm 0.002	0.172 \pm 0.042
	Split	0.556 \pm 0.034	8.3 \pm 0.1	0.036 \pm 0.004	0.252 \pm 0.074
	NCP	0.562 \pm 0.054	7.9 \pm 0.8	0.027 \pm 0.008	0.204 \pm 0.075
	CCP	0.580 \pm 0.044	10.6 \pm 0.8	0.027 \pm 0.005	0.196 \pm 0.027
SAPS	CFCP	0.586 \pm 0.031	8.8 \pm 0.5	0.033 \pm 0.008	0.212 \pm 0.042
	RC3P	0.548 \pm 0.048	10.9 \pm 0.2	0.027 \pm 0.003	0.188 \pm 0.042
	ICP	0.582 \pm 0.051	11.5 \pm 0.2	0.024 \pm 0.003	0.188 \pm 0.042
	Split	0.558 \pm 0.024	8.2 \pm 0.1	0.036 \pm 0.005	0.244 \pm 0.057
	NCP	0.566 \pm 0.078	7.7 \pm 0.8	0.027 \pm 0.011	0.196 \pm 0.057
	CCP	0.568 \pm 0.051	10.3 \pm 0.5	0.028 \pm 0.002	0.204 \pm 0.027
ImageNet					
LAC	CFCP	0.508 \pm 0.004	1.9 \pm 0.0	0.058 \pm 0.001	0.520 \pm 0.000
	RC3P	0.425 \pm 0.009	3.5 \pm 0.1	0.049 \pm 0.001	0.516 \pm 0.122
	ICP	0.493 \pm 0.008	3.9 \pm 0.1	0.038 \pm 0.002	0.484 \pm 0.123
	Split	0.499 \pm 0.005	1.8 \pm 0.0	0.060 \pm 0.001	0.540 \pm 0.000
	NCP	0.494 \pm 0.006	1.9 \pm 0.0	0.063 \pm 0.002	0.500 \pm 0.000
	CCP	0.494 \pm 0.026	3.3 \pm 0.3	0.040 \pm 0.003	0.556 \pm 0.130
APS	CFCP	0.672 \pm 0.002	15.1 \pm 0.2	0.030 \pm 0.000	0.380 \pm 0.000
	RC3P	0.654 \pm 0.008	8.4 \pm 0.5	0.023 \pm 0.001	0.424 \pm 0.062
	ICP	0.658 \pm 0.026	42.8 \pm 0.4	0.019 \pm 0.001	0.240 \pm 0.053
	Split	0.655 \pm 0.008	35.2 \pm 0.3	0.023 \pm 0.001	0.392 \pm 0.028
	NCP	0.667 \pm 0.009	15.2 \pm 0.4	0.033 \pm 0.001	0.448 \pm 0.014
	CCP	0.646 \pm 0.010	38.0 \pm 0.9	0.020 \pm 0.001	0.276 \pm 0.027
RAPS	CFCP	0.589 \pm 0.002	3.6 \pm 0.0	0.042 \pm 0.000	0.440 \pm 0.000
	RC3P	0.546 \pm 0.008	5.9 \pm 0.3	0.033 \pm 0.001	0.444 \pm 0.044
	ICP	0.546 \pm 0.007	5.5 \pm 0.3	0.030 \pm 0.001	0.352 \pm 0.076
	Split	0.553 \pm 0.017	3.3 \pm 0.0	0.039 \pm 0.001	0.404 \pm 0.021
	NCP	0.565 \pm 0.005	2.8 \pm 0.0	0.047 \pm 0.000	0.500 \pm 0.030
	CCP	0.536 \pm 0.035	8.5 \pm 2.4	0.034 \pm 0.003	0.400 \pm 0.058
SAPS	CFCP	0.571 \pm 0.004	2.6 \pm 0.0	0.046 \pm 0.001	0.480 \pm 0.000
	RC3P	0.556 \pm 0.010	6.0 \pm 0.3	0.032 \pm 0.001	0.444 \pm 0.044
	ICP	0.533 \pm 0.021	5.1 \pm 0.2	0.031 \pm 0.001	0.440 \pm 0.053

(continued on next page)

Score	Method	Class Cov. (\uparrow)	Set Size (\downarrow)	WUC (\downarrow)	MaxCE (\downarrow)
<i>(metrics: mean \pm 95 % CI)</i>					
	Split	0.529 \pm 0.007	2.2 \pm 0.0	0.055 \pm 0.000	0.476 \pm 0.032
	NCP	0.559 \pm 0.007	2.4 \pm 0.0	0.049 \pm 0.001	0.448 \pm 0.014
	CCP	0.549 \pm 0.020	6.8 \pm 0.9	0.033 \pm 0.001	0.436 \pm 0.037
ImageNet-V2					
LAC	CFCP	0.446 \pm 0.002	2.5 \pm 0.0	0.128 \pm 0.001	0.900 \pm 0.000
	RC3P	0.424 \pm 0.014	6.9 \pm 0.5	0.125 \pm 0.003	0.720 \pm 0.056
	ICP	0.388 \pm 0.008	5.0 \pm 0.1	0.132 \pm 0.002	0.740 \pm 0.068
	Split	0.452 \pm 0.002	2.4 \pm 0.0	0.128 \pm 0.001	0.900 \pm 0.000
	NCP	0.445 \pm 0.009	2.8 \pm 0.1	0.130 \pm 0.002	0.800 \pm 0.000
	CCP	0.386 \pm 0.019	4.3 \pm 0.2	0.133 \pm 0.006	0.800 \pm 0.124
APS	CFCP	0.714 \pm 0.002	31.2 \pm 0.4	0.046 \pm 0.000	0.500 \pm 0.000
	RC3P	0.712 \pm 0.004	28.1 \pm 1.1	0.047 \pm 0.001	0.560 \pm 0.068
	ICP	0.708 \pm 0.013	72.0 \pm 0.5	0.042 \pm 0.002	0.440 \pm 0.068
	Split	0.710 \pm 0.011	64.7 \pm 0.3	0.043 \pm 0.001	0.520 \pm 0.056
	NCP	0.704 \pm 0.008	39.8 \pm 1.1	0.048 \pm 0.002	0.600 \pm 0.000
	CCP	0.707 \pm 0.019	69.2 \pm 4.1	0.042 \pm 0.003	0.460 \pm 0.068
RAPS	CFCP	0.552 \pm 0.004	4.8 \pm 0.0	0.092 \pm 0.001	0.700 \pm 0.000
	RC3P	0.544 \pm 0.012	10.2 \pm 0.5	0.087 \pm 0.002	0.720 \pm 0.056
	ICP	0.523 \pm 0.007	6.4 \pm 0.1	0.088 \pm 0.001	0.680 \pm 0.056
	Split	0.525 \pm 0.007	4.3 \pm 0.0	0.095 \pm 0.001	0.700 \pm 0.000
	NCP	0.541 \pm 0.006	4.2 \pm 0.0	0.094 \pm 0.001	0.700 \pm 0.000
	CCP	0.529 \pm 0.012	8.8 \pm 1.1	0.087 \pm 0.001	0.680 \pm 0.056
SAPS	CFCP	0.465 \pm 0.002	3.0 \pm 0.0	0.122 \pm 0.001	0.900 \pm 0.000
	RC3P	0.440 \pm 0.008	6.0 \pm 0.3	0.116 \pm 0.002	0.740 \pm 0.068
	ICP	0.463 \pm 0.010	5.5 \pm 0.2	0.104 \pm 0.002	0.720 \pm 0.056
	Split	0.458 \pm 0.003	2.8 \pm 0.0	0.123 \pm 0.001	0.820 \pm 0.056
	NCP	0.446 \pm 0.004	2.8 \pm 0.0	0.125 \pm 0.001	0.800 \pm 0.000
	CCP	0.455 \pm 0.006	7.4 \pm 1.5	0.108 \pm 0.003	0.740 \pm 0.068
WOS-46985					
LAC	CFCP	0.645 \pm 0.031	2.5 \pm 0.3	0.029 \pm 0.005	0.710 \pm 0.135
	RC3P	0.634 \pm 0.054	3.8 \pm 0.6	0.020 \pm 0.002	0.312 \pm 0.082
	ICP	0.621 \pm 0.064	4.1 \pm 0.4	0.021 \pm 0.002	0.312 \pm 0.082
	Split	0.622 \pm 0.017	1.2 \pm 0.0	0.035 \pm 0.003	0.510 \pm 0.188
	NCP	0.619 \pm 0.031	1.3 \pm 0.1	0.027 \pm 0.003	0.810 \pm 0.155
	CCP	0.601 \pm 0.075	5.4 \pm 1.1	0.027 \pm 0.002	0.324 \pm 0.076
APS	CFCP	0.633 \pm 0.018	1.5 \pm 0.0	0.038 \pm 0.003	0.837 \pm 0.107
	RC3P	0.587 \pm 0.052	3.8 \pm 0.5	0.023 \pm 0.002	0.262 \pm 0.113
	ICP	0.606 \pm 0.053	6.2 \pm 0.5	0.020 \pm 0.004	0.278 \pm 0.093
	Split	0.546 \pm 0.034	3.4 \pm 0.2	0.023 \pm 0.004	0.300 \pm 0.113
	NCP	0.609 \pm 0.020	1.5 \pm 0.1	0.036 \pm 0.001	0.475 \pm 0.132
	CCP	0.570 \pm 0.086	6.6 \pm 0.6	0.022 \pm 0.004	0.240 \pm 0.042
RAPS	CFCP	0.633 \pm 0.018	1.5 \pm 0.0	0.038 \pm 0.003	0.837 \pm 0.107
	RC3P	0.579 \pm 0.024	4.0 \pm 0.4	0.020 \pm 0.002	0.261 \pm 0.117
	ICP	0.609 \pm 0.051	5.9 \pm 0.7	0.020 \pm 0.004	0.243 \pm 0.117
	Split	0.560 \pm 0.057	2.8 \pm 0.1	0.021 \pm 0.005	0.300 \pm 0.113
	NCP	0.600 \pm 0.019	1.5 \pm 0.0	0.036 \pm 0.002	0.503 \pm 0.134
	CCP	0.587 \pm 0.047	6.0 \pm 0.6	0.021 \pm 0.005	0.205 \pm 0.030
SAPS	CFCP	0.643 \pm 0.025	2.3 \pm 0.1	0.048 \pm 0.004	0.827 \pm 0.126
	RC3P	0.604 \pm 0.051	3.7 \pm 0.3	0.021 \pm 0.003	0.270 \pm 0.101

SAPS

(continued on next page)

Score	Method	Class Cov. (↑)	Set Size (↓)	WUC (↓)	MaxCE (↓)
<i>(metrics: mean ± 95 % CI)</i>					
	ICP	0.610 ± 0.051	5.8 ± 0.6	0.021 ± 0.003	0.257 ± 0.046
	Split	0.590 ± 0.046	1.3 ± 0.0	0.029 ± 0.002	0.420 ± 0.056
	NCP	0.630 ± 0.037	1.3 ± 0.0	0.029 ± 0.001	0.420 ± 0.056
	CCP	0.604 ± 0.049	5.1 ± 0.8	0.027 ± 0.002	0.282 ± 0.068

Table 4: Within-family comparison of CFCP against baselines at $\alpha = 0.1$. Values are means over five repeated dataset splits. **Bold** marks the best under coverage error within each family. Full results including 95% CIs are in Appendix C.2.

Dataset	Score	CFCP (ours)		Split		ICP		CCP		NCP		RC3P	
		WUC↓	MaxCE↓	WUC↓	MaxCE↓	WUC↓	MaxCE↓	WUC↓	MaxCE↓	WUC↓	MaxCE↓	WUC↓	MaxCE↓
CIFAR-100	LAC	0.030	0.196	0.033	0.228	0.026	0.164	0.027	0.204	0.023	0.164	0.026	0.164
	APS	0.025	0.220	0.032	0.212	0.026	0.188	0.029	0.188	0.024	0.172	0.025	0.196
	RAPS	0.031	0.212	0.036	0.252	0.025	0.172	0.027	0.196	0.027	0.204	0.025	0.172
	SAPS	0.033	0.212	0.036	0.244	0.024	0.188	0.028	0.204	0.027	0.196	0.027	0.188
ImageNet	LAC	0.058	0.520	0.060	0.540	0.038	0.484	0.040	0.556	0.063	0.500	0.049	0.516
	APS	0.030	0.380	0.023	0.392	0.019	0.240	0.020	0.276	0.033	0.448	0.023	0.424
	RAPS	0.042	0.440	0.039	0.404	0.030	0.352	0.034	0.400	0.047	0.500	0.033	0.444
	SAPS	0.046	0.480	0.055	0.476	0.031	0.440	0.033	0.436	0.049	0.448	0.032	0.444
ImageNet-V2	LAC	0.128	0.900	0.128	0.900	0.132	0.740	0.133	0.800	0.130	0.800	0.125	0.720
	APS	0.046	0.500	0.043	0.520	0.042	0.440	0.042	0.460	0.048	0.600	0.047	0.560
	RAPS	0.092	0.700	0.095	0.700	0.088	0.680	0.087	0.680	0.094	0.700	0.087	0.720
	SAPS	0.122	0.900	0.123	0.820	0.104	0.720	0.108	0.740	0.125	0.800	0.116	0.740
WOS-46985	LAC	0.029	0.710	0.035	0.510	0.021	0.312	0.027	0.324	0.027	0.810	0.020	0.312
	APS	0.038	0.837	0.023	0.300	0.020	0.278	0.022	0.240	0.036	0.475	0.023	0.262
	RAPS	0.038	0.837	0.021	0.300	0.020	0.243	0.021	0.205	0.036	0.503	0.020	0.261
	SAPS	0.048	0.827	0.029	0.420	0.021	0.257	0.027	0.282	0.029	0.420	0.021	0.270

Table 5: Example CFCP hyperparameter grid search used in the sensitivity analysis. The table reports top 20 APS configurations across locality-specific hyperparameters on the CIFAR-100 dataset: number of clusters K , number of neighboring centroids m , assignment temperature τ , Dirichlet smoothing β , reliability exponent γ , and support shrinkage β_{sup} . Displayed are our main metrics: missed class coverage (Misses) and average set size, as well as the secondary diagnostics of weighted under-coverage (WUC) and MaxCE. Lower is better for all metrics. The near-best configurations achieve similar class coverage and set size across different hyperparameter choices, illustrating that CFCP is task-adaptive but not brittle to a single finely tuned setting.

K	m	τ	β	γ	β_{sup}	Misses	Size	WUC	MaxCE
120	3	0.08	2	2	150	45.4	8.368	0.028	0.204
120	3	0.08	2	1	150	46.6	7.851	0.028	0.188
120	3	0.12	2	2	150	45.4	8.330	0.028	0.188
120	3	0.08	8	2	150	43.4	9.713	0.028	0.196
120	3	0.12	2	1	150	45.4	7.614	0.029	0.188
120	3	0.08	8	1	40	45.6	8.927	0.029	0.180
120	3	0.08	2	1	40	46.6	8.451	0.029	0.196
120	20	0.08	2	1	40	44.8	8.566	0.029	0.236
120	3	0.08	8	2	40	45.0	11.973	0.029	0.180
120	3	0.08	8	1	150	46.4	8.041	0.029	0.180
120	3	0.12	8	2	150	46.8	10.038	0.029	0.212
120	3	0.08	2	2	40	45.6	9.249	0.030	0.172
120	20	0.08	2	1	150	46.2	7.758	0.030	0.220
120	3	0.12	8	1	40	44.8	8.696	0.030	0.188
80	3	0.08	2	2	0	43.6	10.778	0.030	0.212
120	10	0.08	2	1	150	46.6	7.498	0.030	0.204
120	3	0.12	8	1	0	43.8	10.361	0.030	0.204
80	3	0.08	2	1	40	44.6	8.876	0.030	0.196

Table 6: ImageNet and ImageNet-V2 ablation of CFCP locality. We compare the full CFCP variant using learned clusters and soft assignment ($K = 180, m = 50$), a hard-assignment variant using only the nearest cluster ($K = 180, m = 1$), and a no-cluster variant that uses only the global label-frequency model with shrinkage ($K = 1, m = 1$). Coverage misses denotes the mean number of classes whose empirical class-conditional coverage falls below the target level. Lower is better. Size denotes the mean prediction-set size. Lower is better. The results show that soft cluster assignment gives the strongest coverage-efficiency tradeoff, while removing clusters produces very large prediction sets.

Ablation	Score	Misses	Set Size
ImageNet			
Full CFCP	APS	328	15.1
	LAC	454.4	2.1
	RAPS	326.6	4.5
	SAPS	430.6	2.6
Hard assignment	APS	439.2	29.6
	LAC	430.8	15.5
	RAPS	442.6	15.7
	SAPS	437.2	15.8
No clusters / Global	APS	397.2	340.0
	LAC	396.8	340.3
	RAPS	397.2	340.0
	SAPS	398	340.1
ImageNet-V2			
Full CFCP	APS	286.4	31.2
	LAC	556.2	2.4
	RAPS	433	5.1
	SAPS	546.2	2.9
Hard assignment	APS	543.4	30.8
	LAC	545.8	15.6
	RAPS	557	15.8
	SAPS	552	15.9
No clusters / Global	APS	446.6	340.1
	LAC	447.2	340.4
	RAPS	446.6	340.1
	SAPS	446.2	340.1

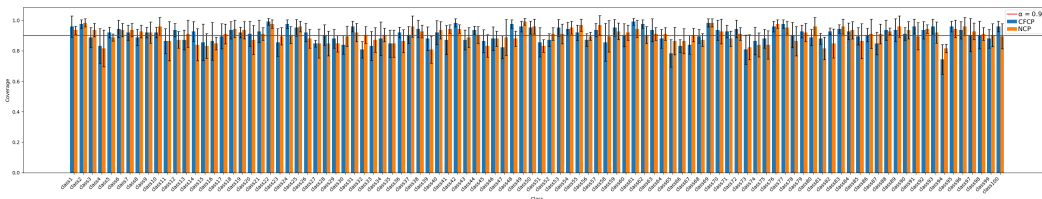
C.3 Failure-mode case study on CIFAR-100

To better understand residual tail failures, we compare CFCP against the closest local-neighborhood baseline, NCP, on CIFAR-100 using APS and RAPS. For each score family, we identify the worst-covered CFCP classes and report their empirical class-conditional coverage, coverage deficit relative to the nominal target $1 - \alpha = 0.9$, class frequency and average prediction-set size. Since CIFAR-100 is class-balanced, all reported classes have the same empirical frequency. Therefore, these failures are not explained by class rarity, but rather by residual representation ambiguity or by the smoothing and global-thresholding components of CFCP.

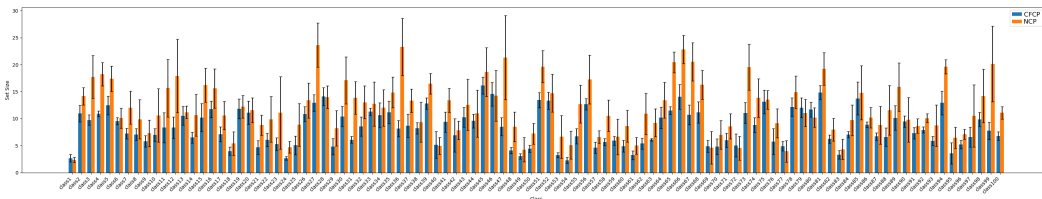
Table 7: CIFAR-100 failure-mode case study comparing CFCP and NCP at $\alpha = 0.1$. Rows show the worst-covered CFCP classes for APS and RAPS, using mean classwise coverage over five splits. $\Delta_{0.9} = [0.9 - \widehat{\text{Cov}}_c]_+$ denotes the classwise under-coverage deficit. Class names follow the standard CIFAR-100 class ordering.

Score	Class	Freq.	Coverage		$\Delta_{0.9}$		Set size	
			CFCP	NCP	CFCP	NCP	CFCP	NCP
APS	class94 (turtle)	1.0%	0.744	0.816	0.156	0.084	12.90	19.62
	class65 (possum)	1.0%	0.784	0.864	0.116	0.036	11.50	20.45
	class32 (elephant)	1.0%	0.808	0.904	0.092	0.000	8.56	13.03
RAPS	class94 (turtle)	1.0%	0.736	0.808	0.164	0.092	9.46	11.56
	class66 (rabbit)	1.0%	0.768	0.872	0.132	0.028	9.50	11.97
	class65 (possum)	1.0%	0.768	0.776	0.132	0.124	9.38	12.49

Table 7 shows that CFCP can improve the broad coverage-efficiency tradeoff while still leaving a small number of classes with larger residual under-coverage. The clearest failure case is class94, which is the worst-covered CFCP class under both APS and RAPS. For APS, CFCP attains substantially smaller sets than NCP for the same classes, but this efficiency is accompanied by a larger worst-class deficit. For RAPS, the same class remains the largest residual failure, although the difference in set size is smaller. Both CFCP and NCP identify the classifier’s low confidence on samples from the under-covered classes, resulting in larger prediction sets. Still, for these classes CFCP exhibits worse coverage due to its residual limitation. These results motivate tail-sensitive extensions of CFCP, such as class or cluster-aware threshold adjustments, while preserving the main empirical advantage of the method: improved class coverage and competitive or smaller prediction sets on average.

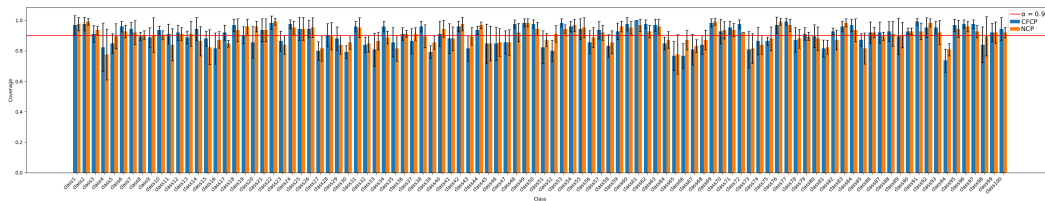


(a) Class-conditional coverage.

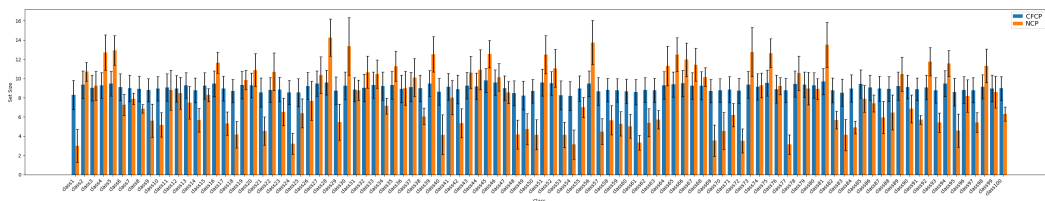


(b) Class-conditional average prediction-set size.

Figure 3: CIFAR-100 classwise comparison of CFCP-APS and NCP-APS at $\alpha = 0.1$. The red horizontal line marks the nominal target coverage $1 - \alpha = 0.9$. CFCP is generally more efficient, but the failure-mode table shows that a few classes retain larger under-coverage deficits.



(a) Class-conditional coverage.



(b) Class-conditional average prediction-set size.

Figure 4: CIFAR-100 classwise comparison of CFCEP-RAPS and NCP-RAPS at $\alpha = 0.1$. CFCEP covers more classes in the mean classwise view, but the worst-covered CFCEP class still has a larger residual under-coverage deficit than the corresponding NCP value.

NeurIPS Paper Checklist

1. Claims

Question: Do the main claims made in the abstract and introduction accurately reflect the paper’s contributions and scope?

Answer: [Yes]

Justification: The abstract and introduction state the paper’s three main contributions: introducing CFCP as a plug-in conformal framework, establishing finite-sample marginal validity in the disjoint-split regime together with an oracle local-validity interpretation for randomized APS, and showing strong empirical class-coverage performance on image and text benchmarks. The paper also states important limitations, including that worst-class max coverage error can remain high on rare classes.

Guidelines:

- The answer [N/A] means that the abstract and introduction do not include the claims made in the paper.
- The abstract and/or introduction should clearly state the claims made, including the contributions made in the paper and important assumptions and limitations. A [No] or [N/A] answer to this question will not be perceived well by the reviewers.
- The claims made should match theoretical and experimental results, and reflect how much the results can be expected to generalize to other settings.
- It is fine to include aspirational goals as motivation as long as it is clear that these goals are not attained by the paper.

2. Limitations

Question: Does the paper discuss the limitations of the work performed by the authors?

Answer: [Yes]

Justification: Section 5 discusses limitations. It notes that CFCP smooths across nearby clusters with a single global threshold, which can dilute very rare or atypical classes, leading to worse max coverage error on a small number of hard classes. Section 5 also outlines future directions including tail-sensitive extensions. A Failure-mode case study is available in Appendix C.3.

Guidelines:

- The answer [N/A] means that the paper has no limitation while the answer [No] means that the paper has limitations, but those are not discussed in the paper.
- The authors are encouraged to create a separate “Limitations” section in their paper.
- The paper should point out any strong assumptions and how robust the results are to violations of these assumptions (e.g., independence assumptions, noiseless settings, model well-specification, asymptotic approximations only holding locally). The authors should reflect on how these assumptions might be violated in practice and what the implications would be.
- The authors should reflect on the scope of the claims made, e.g., if the approach was only tested on a few datasets or with a few runs. In general, empirical results often depend on implicit assumptions, which should be articulated.
- The authors should reflect on the factors that influence the performance of the approach. For example, a facial recognition algorithm may perform poorly when image resolution is low or images are taken in low lighting. Or a speech-to-text system might not be used reliably to provide closed captions for online lectures because it fails to handle technical jargon.
- The authors should discuss the computational efficiency of the proposed algorithms and how they scale with dataset size.
- If applicable, the authors should discuss possible limitations of their approach to address problems of privacy and fairness.
- While the authors might fear that complete honesty about limitations might be used by reviewers as grounds for rejection, a worse outcome might be that reviewers discover limitations that aren’t acknowledged in the paper. The authors should use their best

judgment and recognize that individual actions in favor of transparency play an important role in developing norms that preserve the integrity of the community. Reviewers will be specifically instructed to not penalize honesty concerning limitations.

3. Theory assumptions and proofs

Question: For each theoretical result, does the paper provide the full set of assumptions and a complete (and correct) proof?

Answer: [Yes]

Justification: Section 3 states the main theoretical results (Theorem 1, Corollary 1, Corollary 2) with their assumptions clearly listed. Full proofs are provided in Appendix B, including the marginal validity proof (Appendix B.1, Theorem 1 and Corollary 1), the oracle local validity proof for randomized APS (Appendix B.2, Lemma 2 and Theorem 3), and the approximate local validity proposition (Appendix B.3, Proposition 1). Theorem 3 and Corollary 2 provide the oracle information advantage result. All theorems and lemmas are numbered and cross-referenced.

Guidelines:

- The answer [N/A] means that the paper does not include theoretical results.
- All the theorems, formulas, and proofs in the paper should be numbered and cross-referenced.
- All assumptions should be clearly stated or referenced in the statement of any theorems.
- The proofs can either appear in the main paper or the supplemental material, but if they appear in the supplemental material, the authors are encouraged to provide a short proof sketch to provide intuition.
- Inversely, any informal proof provided in the core of the paper should be complemented by formal proofs provided in appendix or supplemental material.
- Theorems and Lemmas that the proof relies upon should be properly referenced.

4. Experimental result reproducibility

Question: Does the paper fully disclose all the information needed to reproduce the main experimental results of the paper to the extent that it affects the main claims and/or conclusions of the paper (regardless of whether the code and data are provided or not)?

Answer: [Yes]

Justification: Section 4 specifies all datasets, architectures, baseline methods and coverage level. Appendix C.1 provides full experimental details on method parameters, data splits, model training (including optimizer settings, learning rates, and epochs), and baseline hyperparameter grids. The paper also provides the code for reproducing all experiments. All results are reported as means over five repeated dataset splits with fixed seeds.

Guidelines:

- The answer [N/A] means that the paper does not include experiments.
- If the paper includes experiments, a [No] answer to this question will not be perceived well by the reviewers: Making the paper reproducible is important, regardless of whether the code and data are provided or not.
- If the contribution is a dataset and/or model, the authors should describe the steps taken to make their results reproducible or verifiable.
- Depending on the contribution, reproducibility can be accomplished in various ways. For example, if the contribution is a novel architecture, describing the architecture fully might suffice, or if the contribution is a specific model and empirical evaluation, it may be necessary to either make it possible for others to replicate the model with the same dataset, or provide access to the model. In general, releasing code and data is often one good way to accomplish this, but reproducibility can also be provided via detailed instructions for how to replicate the results, access to a hosted model (e.g., in the case of a large language model), releasing of a model checkpoint, or other means that are appropriate to the research performed.
- While NeurIPS does not require releasing code, the conference does require all submissions to provide some reasonable avenue for reproducibility, which may depend on the nature of the contribution. For example

- (a) If the contribution is primarily a new algorithm, the paper should make it clear how to reproduce that algorithm.
- (b) If the contribution is primarily a new model architecture, the paper should describe the architecture clearly and fully.
- (c) If the contribution is a new model (e.g., a large language model), then there should either be a way to access this model for reproducing the results or a way to reproduce the model (e.g., with an open-source dataset or instructions for how to construct the dataset).
- (d) We recognize that reproducibility may be tricky in some cases, in which case authors are welcome to describe the particular way they provide for reproducibility. In the case of closed-source models, it may be that access to the model is limited in some way (e.g., to registered users), but it should be possible for other researchers to have some path to reproducing or verifying the results.

5. Open access to data and code

Question: Does the paper provide open access to the data and code, with sufficient instructions to faithfully reproduce the main experimental results, as described in supplemental material?

Answer: [Yes]

Justification: Code for reproducing all experiments and summary results is available at an anonymous repository. The repository includes a README with instructions and a license. All datasets used (CIFAR-100, ImageNet, ImageNet-V2, WOS-46985) are publicly available benchmarks.

Guidelines:

- The answer [N/A] means that paper does not include experiments requiring code.
- Please see the NeurIPS code and data submission guidelines (<https://neurips.cc/public/guides/CodeSubmissionPolicy>) for more details.
- While we encourage the release of code and data, we understand that this might not be possible, so [No] is an acceptable answer. Papers cannot be rejected simply for not including code, unless this is central to the contribution (e.g., for a new open-source benchmark).
- The instructions should contain the exact command and environment needed to run to reproduce the results. See the NeurIPS code and data submission guidelines (<https://neurips.cc/public/guides/CodeSubmissionPolicy>) for more details.
- The authors should provide instructions on data access and preparation, including how to access the raw data, preprocessed data, intermediate data, and generated data, etc.
- The authors should provide scripts to reproduce all experimental results for the new proposed method and baselines. If only a subset of experiments are reproducible, they should state which ones are omitted from the script and why.
- At submission time, to preserve anonymity, the authors should release anonymized versions (if applicable).
- Providing as much information as possible in supplemental material (appended to the paper) is recommended, but including URLs to data and code is permitted.

6. Experimental setting/details

Question: Does the paper specify all the training and test details (e.g., data splits, hyperparameters, how they were chosen, type of optimizer) necessary to understand the results?

Answer: [Yes]

Justification: Section 4 describes datasets, model architectures, learned representations, baseline methods, coverage level and statistical significance methodology. Appendix C.1 provides the complete experimental setup for each dataset, including method parameters, data splits, model architectures, pre-training strategies, fine-tuning hyperparameters (learning rate, weight decay, warmup ratio, epochs), and CFCP-specific hyperparameter grids.

Guidelines:

- The answer [N/A] means that the paper does not include experiments.

- The experimental setting should be presented in the core of the paper to a level of detail that is necessary to appreciate the results and make sense of them.
- The full details can be provided either with the code, in appendix, or as supplemental material.

7. Experiment statistical significance

Question: Does the paper report error bars suitably and correctly defined or other appropriate information about the statistical significance of the experiments?

Answer: [Yes]

Justification: All reported results are means over five repeated dataset splits with fixed seeds and 95% confidence intervals are computed (Section 4). The 95% CIs are omitted from the main tables for readability and are available in Appendix C.2 with the full experimental results.

Guidelines:

- The answer [N/A] means that the paper does not include experiments.
- The authors should answer [Yes] if the results are accompanied by error bars, confidence intervals, or statistical significance tests, at least for the experiments that support the main claims of the paper.
- The factors of variability that the error bars are capturing should be clearly stated (for example, train/test split, initialization, random drawing of some parameter, or overall run with given experimental conditions).
- The method for calculating the error bars should be explained (closed form formula, call to a library function, bootstrap, etc.)
- The assumptions made should be given (e.g., Normally distributed errors).
- It should be clear whether the error bar is the standard deviation or the standard error of the mean.
- It is OK to report 1-sigma error bars, but one should state it. The authors should preferably report a 2-sigma error bar than state that they have a 96% CI, if the hypothesis of Normality of errors is not verified.
- For asymmetric distributions, the authors should be careful not to show in tables or figures symmetric error bars that would yield results that are out of range (e.g., negative error rates).
- If error bars are reported in tables or plots, the authors should explain in the text how they were calculated and reference the corresponding figures or tables in the text.

8. Experiments compute resources

Question: For each experiment, does the paper provide sufficient information on the computer resources (type of compute workers, memory, time of execution) needed to reproduce the experiments?

Answer: [Yes]

Justification: Appendix C.1 states that all experiments were performed on a MacBook Pro M4 Max with 36GB RAM. Section 3.1 and Appendix A.4 discuss the computational complexity of CFCP, including the time complexity of clustering and nearest-centroid retrieval. A full run of all reported CFCP experiments required approximately 3-4 hours. Individual dataset runs required approximately 30-60 minutes depending on the dataset.

Guidelines:

- The answer [N/A] means that the paper does not include experiments.
- The paper should indicate the type of compute workers CPU or GPU, internal cluster, or cloud provider, including relevant memory and storage.
- The paper should provide the amount of compute required for each of the individual experimental runs as well as estimate the total compute.
- The paper should disclose whether the full research project required more compute than the experiments reported in the paper (e.g., preliminary or failed experiments that didn't make it into the paper).

9. Code of ethics

Question: Does the research conducted in the paper conform, in every respect, with the NeurIPS Code of Ethics <https://neurips.cc/public/EthicsGuidelines>?

Answer: [Yes]

Justification: The research conforms with the NeurIPS Code of Ethics. The paper uses only publicly available benchmark datasets, does not involve human subjects, and the proposed method is a general-purpose improvement to conformal prediction that does not raise specific ethical concerns.

Guidelines:

- The answer [N/A] means that the authors have not reviewed the NeurIPS Code of Ethics.
- If the authors answer [No], they should explain the special circumstances that require a deviation from the Code of Ethics.
- The authors should make sure to preserve anonymity (e.g., if there is a special consideration due to laws or regulations in their jurisdiction).

10. Broader impacts

Question: Does the paper discuss both potential positive societal impacts and negative societal impacts of the work performed?

Answer: [Yes]

Justification: CFCP may improve reliability in high-stakes classification settings by reducing classwise coverage disparities. However, it does not guarantee exact coverage for every subgroup, and the failure-mode analysis shows that some hard classes may remain under-covered. Therefore, CFCP should not be used as a standalone safety guarantee in medical, legal, or other high-stakes deployments without domain-specific validation and monitoring.

Guidelines:

- The answer [N/A] means that there is no societal impact of the work performed.
- If the authors answer [N/A] or [No], they should explain why their work has no societal impact or why the paper does not address societal impact.
- Examples of negative societal impacts include potential malicious or unintended uses (e.g., disinformation, generating fake profiles, surveillance), fairness considerations (e.g., deployment of technologies that could make decisions that unfairly impact specific groups), privacy considerations, and security considerations.
- The conference expects that many papers will be foundational research and not tied to particular applications, let alone deployments. However, if there is a direct path to any negative applications, the authors should point it out. For example, it is legitimate to point out that an improvement in the quality of generative models could be used to generate Deepfakes for disinformation. On the other hand, it is not needed to point out that a generic algorithm for optimizing neural networks could enable people to train models that generate Deepfakes faster.
- The authors should consider possible harms that could arise when the technology is being used as intended and functioning correctly, harms that could arise when the technology is being used as intended but gives incorrect results, and harms following from (intentional or unintentional) misuse of the technology.
- If there are negative societal impacts, the authors could also discuss possible mitigation strategies (e.g., gated release of models, providing defenses in addition to attacks, mechanisms for monitoring misuse, mechanisms to monitor how a system learns from feedback over time, improving the efficiency and accessibility of ML).

11. Safeguards

Question: Does the paper describe safeguards that have been put in place for responsible release of data or models that have a high risk for misuse (e.g., pre-trained language models, image generators, or scraped datasets)?

Answer: [N/A]

Justification: The paper does not release pre-trained models, generated data, or scraped datasets. CFCP is a plug-in conformal prediction method that operates on top of existing

classifiers and uses only publicly available benchmark datasets. The released code poses no risk for misuse.

Guidelines:

- The answer [N/A] means that the paper poses no such risks.
- Released models that have a high risk for misuse or dual-use should be released with necessary safeguards to allow for controlled use of the model, for example by requiring that users adhere to usage guidelines or restrictions to access the model or implementing safety filters.
- Datasets that have been scraped from the Internet could pose safety risks. The authors should describe how they avoided releasing unsafe images.
- We recognize that providing effective safeguards is challenging, and many papers do not require this, but we encourage authors to take this into account and make a best faith effort.

12. Licenses for existing assets

Question: Are the creators or original owners of assets (e.g., code, data, models), used in the paper, properly credited and are the license and terms of use explicitly mentioned and properly respected?

Answer: [Yes]

Justification: The original papers for all datasets (CIFAR-100, ImageNet, ImageNet-V2, WOS-46985), pre-trained models (ResNet-50, DistilBERT, SimCLR-v2), and software libraries (PyTorch, TorchCP, FAISS) are properly cited, including license indication.

Guidelines:

- The answer [N/A] means that the paper does not use existing assets.
- The authors should cite the original paper that produced the code package or dataset.
- The authors should state which version of the asset is used and, if possible, include a URL.
- The name of the license (e.g., CC-BY 4.0) should be included for each asset.
- For scraped data from a particular source (e.g., website), the copyright and terms of service of that source should be provided.
- If assets are released, the license, copyright information, and terms of use in the package should be provided. For popular datasets, paperswithcode.com/datasets has curated licenses for some datasets. Their licensing guide can help determine the license of a dataset.
- For existing datasets that are re-packaged, both the original license and the license of the derived asset (if it has changed) should be provided.
- If this information is not available online, the authors are encouraged to reach out to the asset's creators.

13. New assets

Question: Are new assets introduced in the paper well documented and is the documentation provided alongside the assets?

Answer: [Yes]

Justification: The released code repository includes a README with usage instructions and a license file. The paper provides the full algorithmic specification in Section 2 and Appendix A, which together with the code enable reproduction of all results.

Guidelines:

- The answer [N/A] means that the paper does not release new assets.
- Researchers should communicate the details of the dataset/code/model as part of their submissions via structured templates. This includes details about training, license, limitations, etc.
- The paper should discuss whether and how consent was obtained from people whose asset is used.

- At submission time, remember to anonymize your assets (if applicable). You can either create an anonymized URL or include an anonymized zip file.

14. Crowdsourcing and research with human subjects

Question: For crowdsourcing experiments and research with human subjects, does the paper include the full text of instructions given to participants and screenshots, if applicable, as well as details about compensation (if any)?

Answer: [N/A]

Justification: The paper does not involve crowdsourcing or research with human subjects.

Guidelines:

- The answer [N/A] means that the paper does not involve crowdsourcing nor research with human subjects.
- Including this information in the supplemental material is fine, but if the main contribution of the paper involves human subjects, then as much detail as possible should be included in the main paper.
- According to the NeurIPS Code of Ethics, workers involved in data collection, curation, or other labor should be paid at least the minimum wage in the country of the data collector.

15. Institutional review board (IRB) approvals or equivalent for research with human subjects

Question: Does the paper describe potential risks incurred by study participants, whether such risks were disclosed to the subjects, and whether Institutional Review Board (IRB) approvals (or an equivalent approval/review based on the requirements of your country or institution) were obtained?

Answer: [N/A]

Justification: The paper does not involve crowdsourcing or research with human subjects.

Guidelines:

- The answer [N/A] means that the paper does not involve crowdsourcing nor research with human subjects.
- Depending on the country in which research is conducted, IRB approval (or equivalent) may be required for any human subjects research. If you obtained IRB approval, you should clearly state this in the paper.
- We recognize that the procedures for this may vary significantly between institutions and locations, and we expect authors to adhere to the NeurIPS Code of Ethics and the guidelines for their institution.
- For initial submissions, do not include any information that would break anonymity (if applicable), such as the institution conducting the review.

16. Declaration of LLM usage

Question: Does the paper describe the usage of LLMs if it is an important, original, or non-standard component of the core methods in this research? Note that if the LLM is used only for writing, editing, or formatting purposes and does *not* impact the core methodology, scientific rigor, or originality of the research, declaration is not required.

Answer: [N/A]

Justification: The core method development in this research does not involve LLMs as any important, original, or non-standard component. CFCP operates on learned representations from standard classifiers (ResNet-50, DistilBERT, SimCLR-v2) and does not use LLMs in its methodology.

Guidelines:

- The answer [N/A] means that the core method development in this research does not involve LLMs as any important, original, or non-standard components.
- Please refer to our LLM policy in the NeurIPS handbook for what should or should not be described.